

Novel Antimalarial Tetrazoles and Amides Active against the Hemoglobin Degradation Pathway in *Plasmodium falciparum*

Aloysus Lawong, Suraksha Gahalawat, John Okombo, Josefine Striepen, Tomas Yeo, Sachel Mok, Ioanna Deni, Jessica L. Bridgford, Hanspeter Niederstrasser, Anwu Zhou, Bruce Posner, Sergio Wittlin, Francisco Javier Gamo, Benigno Crespo, Alisje Churchyard, Jake Baum, Nimisha Mittal, Elizabeth Winzeler, Benoît Laleu, Michael J. Palmer, Susan A. Charman, David A. Fidock, Joseph M. Ready,* and Margaret A. Phillips*



Cite This: *J. Med. Chem.* 2021, 64, 2739–2761



Read Online

ACCESS |



Metrics & More

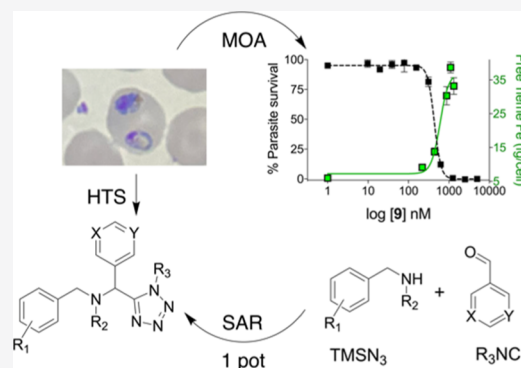


Article Recommendations



Supporting Information

ABSTRACT: Malaria control programs continue to be threatened by drug resistance. To identify new antimalarials, we conducted a phenotypic screen and identified a novel tetrazole-based series that shows fast-kill kinetics and a relatively low propensity to develop high-level resistance. Preliminary structure–activity relationships were established including identification of a subseries of related amides with antiplasmodial activity. Assaying parasites with resistance to antimalarials led us to test whether the series had a similar mechanism of action to chloroquine (CQ). Treatment of synchronized *Plasmodium falciparum* parasites with active analogues revealed a pattern of intracellular inhibition of hemozoin (Hz) formation reminiscent of CQ's action. Drug selections yielded only modest resistance that was associated with amplification of the multidrug resistance gene 1 (*pfmdr1*). Thus, we have identified a novel chemical series that targets the historically druggable heme polymerization pathway and that can form the basis of future optimization efforts to develop a new malaria treatment.



INTRODUCTION

Malaria remains a leading cause of mortality and morbidity worldwide. Global malaria deaths in 2020 were estimated at ~0.4 million, with African children under the age of 5 representing the most vulnerable demographic and accounting for 272,000 (67%) of all malaria deaths.¹ An estimated 228 million cases occurred worldwide in the same period. In high-burden countries, malaria continues to place a significant strain on healthcare systems, while leading to substantial losses in economic output, creating a cycle of poverty. The causative agent of malaria is an obligate intracellular parasite from the *Plasmodium* genus, of which there are five human infective species. *Plasmodium falciparum* and *Plasmodium vivax* account for most cases of malaria, with the former responsible for almost all malaria deaths.²

A number of drugs with a range of modes of action (MOA) have been used to treat malaria, including chloroquine (CQ), which became the mainstay of treatment and prevention programs in the late 1940s.³ Widespread *P. falciparum* resistance to CQ led to its loss of efficacy, a fate shared by sulfadoxine + pyrimethamine (which inhibit dihydropteroate synthase and dihydrofolate reductase, respectively) that was introduced in the late 1950s. Parasite resistance extends to nearly every other drug

that has been used in malaria treatment programs.⁴ The introduction of artemisinin-based combination therapies (ACTs) as the first-line treatment regimen restored effective malaria control, and their use has led to substantial reductions in malaria disease burden in the last two decades.⁵ However, increasing ACT treatment failure rates are being reported, particularly in the Greater Mekong Subregion. *P. falciparum* resistance to artemisinin (ART) is associated with mutations in Kelch13 and with delayed parasite clearance times.^{6–9} These reductions in ART potency have paralleled the emergence of resistance to partner compounds,¹⁰ further jeopardizing the efficacy of first-line antimalarials and foreshadowing a reversal of the gains made in the last decade.⁵ New challenges in emerging resistance to the current frontline therapies make the discovery of novel antimalarials a critical component to sustaining and improving malaria control programs.

Received: November 21, 2020

Published: February 23, 2021



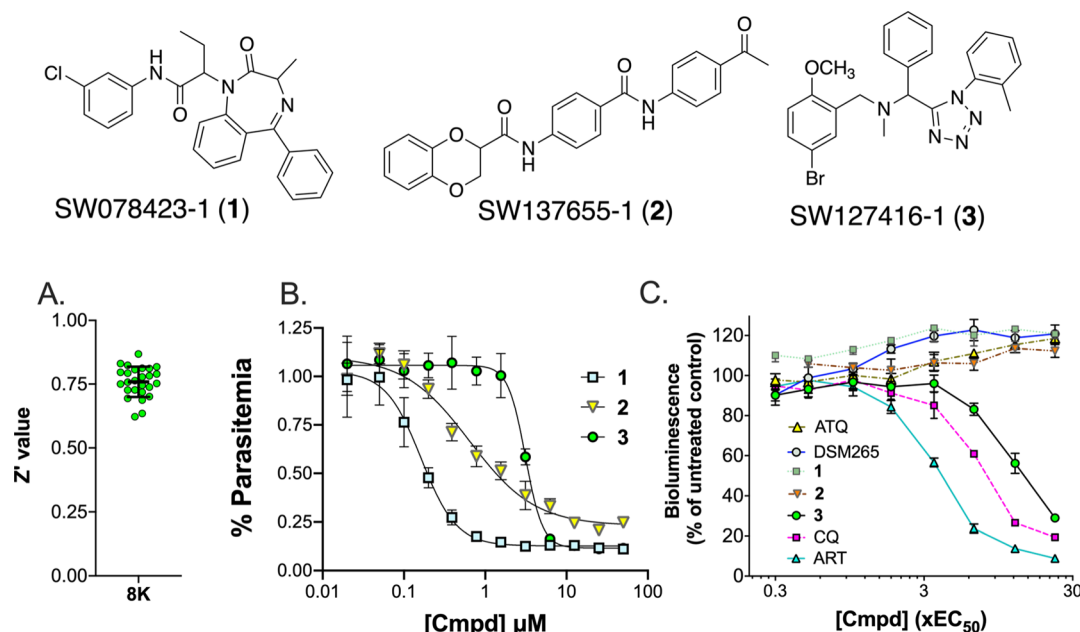


Figure 1. HTS-based identification of compounds that inhibit growth of *P. falciparum* 3D7 ABS parasites. (A) Range of Z' values observed for 384-well plates covering the 8K screening library. The black bar shows the mean \pm standard deviation (std dev). (B) Representative concentration response curves for validated hits vs 3D7 parasites. Data for each drug concentration were collected in triplicate wells, and error bars represent the std dev. Data were fitted to the $\log(I)$ vs response—four-parameter variable slope equation in GraphPad Prism. Replicate data were subsequently collected, yielding the following EC_{50} 's: 1, $0.31 \pm 0.10 \mu\text{M}$; 2, $0.71 \pm 0.075 \mu\text{M}$; and 3, $3.5 \pm 0.71 \mu\text{M}$, where errors are the std dev for at least three independent biological replicates. (C) BRROK rate of kill assay. Serial log-fold dilutions of compounds from $30\times EC_{50}$ to $0.33\times EC_{50}$ were incubated for 6 h with NF54-luc parasites, and viability was assessed by bioluminescence at the end of the incubation. Bioluminescence signals normalized to untreated controls are plotted and represent mean \pm std dev from triplicate wells. EC_{50} values against 3D7 parasites were determined in standard 72 h SYBR Green assays prior to the start of the study and were used as indicated for compounds 1–3. Benchmark compounds included artemisinin, ART (fast-kill) ($EC_{50} = 0.013 \mu\text{M}$), chloroquine, CQ (fast-kill) ($EC_{50} = 0.014 \mu\text{M}$), atovaquone, ATQ (slow-kill) ($EC_{50} = 0.0013 \mu\text{M}$), and DSM265 (slow-kill) ($EC_{50} = 0.0050 \mu\text{M}$), with EC_{50} values used to calculate compound concentrations for the study indicated in parenthesis. Similar EC_{50} values were obtained versus NF54-luc parasites using bioluminescence as a readout in a 72 h assay (Table S1).

Academic and commercial antimalarial high-throughput screening (HTS) campaigns have leveraged whole cell-based approaches to identify novel antimalarial candidates, some currently in clinical development.^{2,11,12} Early phenotypic screening campaigns focused on targeting asexual blood stage (ABS) parasites, which cause clinical symptoms. This approach led to the identification of several clinical candidates for the treatment of malaria, including the spiroindolone ATP4 inhibitor KAE609 (NITD609),^{13,14} the imidazolopiperazine, KAF156,^{15,16} and PI4 kinase inhibitors^{17,18} including KDU691 and MMV390048. More recent approaches have since allowed development of screening platforms targeting multiple stages of the *Plasmodium* life cycle.^{19–21} These phenotypic screening efforts, combined with the use of forward genetics and whole-genome sequencing (WGS), have proven powerful in identifying the protein targets of antimalarial compounds, including for several of these current development candidates.^{22,23} Target-based screens, including those against dihydroorotate dehydrogenase that led to the identification of DSM265,^{24,25} have also been deployed but so far have led to fewer development candidates than the phenotypic approach.

Herein, we describe the identification of a novel tetrazole-based series from a phenotypic screen against *P. falciparum* ABS parasites (using the 3D7 strain). This series shows a fast kill rate *in vitro*, and life-cycle profiling reveals it to be ABS-specific. Synthesis and evaluation of additional analogues in the series have established preliminary structure–activity relationships (SARs). MOA studies suggest that parasite killing is mediated by inhibition of hemozoin (Hz) formation and the toxic buildup of

free heme in the parasite digestive vacuole (DV), similar to CQ. Selections for resistant parasites have yielded only low-level resistance, and WGS reveals amplification of the multidrug resistance 1 gene (*pfmdr1*). We have thus identified a novel class of antimalarial compounds with a fast-kill mechanism and low resistance propensity and whose MOA appears to involve inhibition of heme detoxification, a critical pathway in the parasite's intraerythrocytic development and a well-validated antimalarial target. These compounds also have the advantage of rapid synthesis from readily available starting materials.

RESULTS

Phenotypic Screen to Identify Novel Compounds Active against *P. falciparum* ABS Parasites. A single-point ($5 \mu\text{M}$) primary screen of an 8K subset of our larger library was executed in a high-throughput optimized 384-well format against the pan-susceptible *P. falciparum* 3D7 strain of ABS parasites, using a published SYBR Green assay.^{26,27} The assay was highly robust, with an average Z' of 0.76 ± 0.059 (where >0.5 is considered a robust assay) across all plates (Figure 1A). We identified a total of 79 hits based on an RZ score cutoff of <-3 . The RZ score represents the number of robust standard deviations (RSD) from the corrected median of a measurement for a library compound, as determined after correction for systematic errors (plate, row, and column effects).^{28,29} Compounds with structural alerts (e.g., PAINS compounds³⁰) or poor drug-like properties³¹ were removed, and a secondary screen at three concentrations (5 , 1.7 , and $0.42 \mu\text{M}$) was performed, yielding 38 confirmed hits. We prioritized

compounds with EC_{50} values $<3 \mu\text{M}$ against 3D7 parasites and selected for chemical novelty based on PubChem and SciFinder(R) searches, while deprioritizing hits that have been previously reported in other malaria screening programs. From our initial hits, we selected three chemotypes (1, 2, and 3) for commercial resupply and evaluated them in 10-point concentration response assays against 3D7 parasites (Figure 1B). These compounds ranged in potency on 3D7 from 0.31 to $3.5 \mu\text{M}$, with 1 showing the best potency [EC_{50} values of $0.31 \mu\text{M}$ (1), $0.71 \mu\text{M}$ (2), and $3.5 \mu\text{M}$ (3)] (Figure 1 legend). Cytotoxicity was assessed against HepG2 cells, with all three compounds showing a $CC_{50} >30 \mu\text{M}$ in this assay.

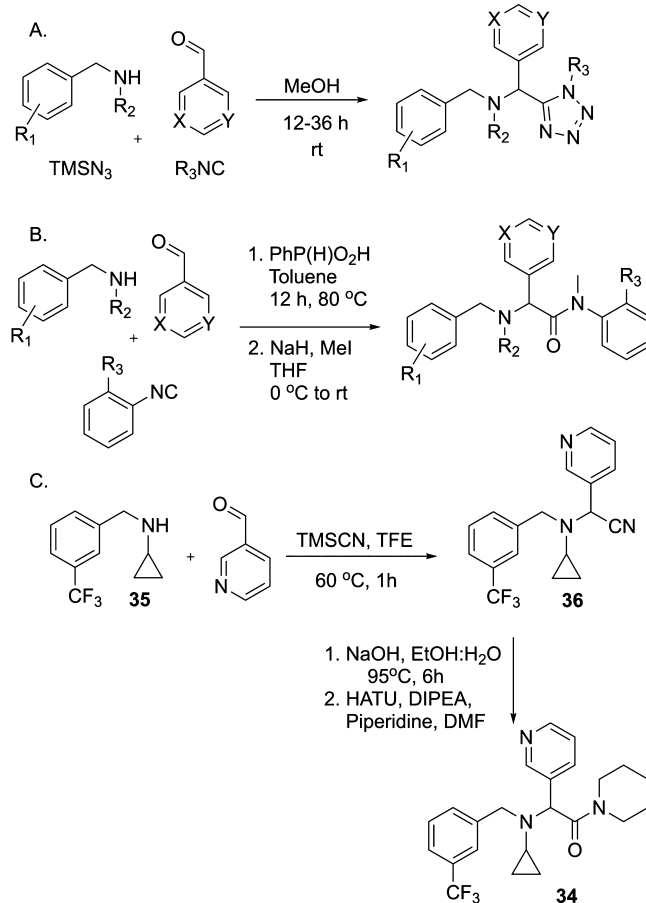
Compounds that show fast kill kinetics are being sought because they provide rapid relief of symptoms, and a more rapid reduction in parasite numbers may also reduce the propensity for resistance to develop.^{32,33} Kill rates also provide information about the MOA as the kill rate has been shown to be a property of the target.³⁴ To this end, compounds were profiled to estimate the rate of kill (Figure 1C) using a rapid bioluminescence relative rate of kill (BRRoK) assay.³⁵ This method follows bioluminescence in a cytotoxic 6 h exposure assay over multiple drug concentrations using a *P. falciparum* strain (*Pf*NF54^{luc})³⁶ that expresses luciferase. We benchmarked the assay against the known fast- (ART and CQ) or slow [DSM265²⁵ and atovaquone (ATQ)]-acting compounds previously characterized using the standard parasite reduction rate (PRR) assay, which measures viability after treatment and regrowth over 28 days.³⁴ In the BRRoK assay, both 1 and 2 showed slow kill kinetics similar to DSM265 and ATQ, while the profile for 3 was similar to CQ and thus consistent with a fast kill mechanism. Based on this desirable property, the 3-series was selected for more in-depth profiling despite lower potency compared to 1 and 2.

Chemistry. Tetrazoles were synthesized using a one-pot, four-component Ugi coupling in the racemic form³⁷ (Scheme 1A). An amine, aldehyde, isocyanate, and trimethylsilyl azide were combined in methanol and stirred for 12–36 h at room temperature (RT) to provide the corresponding coupling product in high yields. In several cases, the enantiomers were separated by preparative high-performance liquid chromatography (HPLC) using a chiral stationary phase. Similarly, most amides were prepared through a three-component Ugi coupling, featuring phenyl phosphinic acid³⁸ (Scheme 1B). The resulting secondary amides were alkylated using methyl iodide in the presence of sodium hydride. Finally, amide 34 was prepared via a Strecker reaction involving 3-pyridine carboxaldehyde and amine 35. Nitrile hydrolysis under basic conditions and amide coupling provided product 34 in high yield (Scheme 1C).

Medicinal Chemistry to Establish SAR of the 3-Series. The 3-series is chemically attractive, with a basic amine, a stable heterocycle, and four vectors for optimization. Initial SAR of the 3-series was established through the synthesis and testing of 19 tetrazole analogues against two strains of *P. falciparum*. These included the 3D7 strain that is broadly drug-sensitive and the Dd2 strain that is resistant to chloroquine and partially resistant to mefloquine (MFQ) and quinine.^{39,40} Compounds were also tested against human HepG2 cells to evaluate cytotoxicity. This work identified compounds with improved potency versus 3D7 of 10- to 20-fold (Table 1).

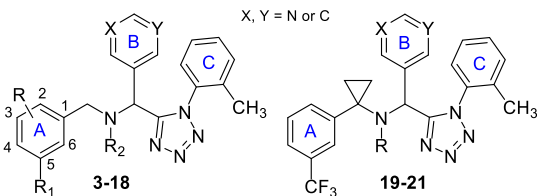
On the A-ring, the Br could be replaced with CF_3 to give 5 with a slight improvement in activity, while removing the Br decreased activity by a factor of 3 (4). Removing the A-ring altogether resulted in an inactive analogue (data not shown).

Scheme 1. Synthesis of Antimalarial Compounds



Replacing the B-ring phenyl with 3-pyridine (3-Py) further improved activity to $\sim 1 \mu\text{M}$ (6), while also improving drug-like properties. The *N*-methyl at the R2 position could be replaced by cyclopropyl (cPr) (7), yielding an additional threefold improvement in potency against 3D7. The OMe on the A-ring could be replaced by F (8) or H (9) without loss of activity. Further modification of the B-ring showed that the 3-Py of 9 could be replaced by a 5-substituted pyrimidine (5-Pyr, 10) with similar activity against 3D7. Introduction of fluoro on the A-ring was also well tolerated at the 3 (11), 4 (12), and 6 (13) positions on the ring. The B-ring could not be replaced with a small nonaromatic cPr ring (14), and a basic amine appeared important because the R2 alkyl group could not be replaced with COCH_3 (15). In contrast, the C-ring could be replaced by either cyclohexyl (17) or cPr (18) with only a two- or threefold loss of activity against 3D7 compared to compounds with matched R2 and B rings, 16 or 9, respectively. However, within the context of the cPr in the C-ring position, the addition of a 2-Me to the B-ring 3-Py was not tolerated (19). The benzylic carbon between the A ring and the tertiary amine could be substituted with a cPr to block a potential site of metabolism. When combined with a propyl (Pr) at R2, these compounds yielded the most potent of the tetrazole series (20 and 21) (3D7 EC_{50} 's $\sim 0.3 \mu\text{M}$, Table 1), representing a 10-fold improvement over the initial hit 3.

Three analogues were selected for separation and evaluation of enantiomer pairs. A small two- to threefold difference in potency was observed between the separated 3-enantiomers [(+)-3 vs (−)-3], while the enantiomers of 6 [(+)-6 and (−)-6]

Table 1. SAR of the Tetrazole Series^a


cmpd	R	R1	R2	B-ring	C-ring	<i>P. falciparum</i> EC ₅₀ (μM)		cytotox CC ₅₀ (μM) HepG2
						Pf3D7	PfDd2	
3	2-OCH ₃	Br	CH ₃	Ph	<i>o</i> -tol	3.5 ± 0.71 (10)	5.4 ± 0.78 (5)	>30
(+)-3	2-OCH ₃	Br	CH ₃	Ph	<i>o</i> -tol	1.5, 1.9	3.0	ND
(-)-3	2-OCH ₃	Br	CH ₃	Ph	<i>o</i> -tol	4.6, 4.4	4.0	ND
4	2-OCH ₃	H	CH ₃	Ph	<i>o</i> -tol	9.7 ± 3.0 (3)	10 ± 1.5 (3)	ND
5	2-OCH ₃	CF ₃	CH ₃	Ph	<i>o</i> -tol	1.7 ± 0.67 (4)	3.7 ± 0.25 (3)	ND
6	2-OCH ₃	CF ₃	CH ₃	3-Py	<i>c</i> -tol	1.3 ± 0.12 (3)	2.3 ± 0.40 (3)	ND
(+)-6	2-OCH ₃	CF ₃	CH ₃	3-Py	<i>c</i> -tol	1.6, 1.5	2.5	ND
(-)-6	2-OCH ₃	CF ₃	CH ₃	3-Py	<i>o</i> -tol	1.2, 1.2	1.7	ND
7	2-OCH ₃	CF ₃	<i>c</i> Pr	3-Py	<i>o</i> -tol	0.49 ± 0.10 (3)	0.48 ± 0.029 (3)	16
8	2-F	CF ₃	<i>c</i> Pr	3-Py	<i>o</i> -tol	0.60 ± 0.17 (3)	0.67 ± 0.031 (3)	ND
9	H	CF ₃	<i>c</i> Pr	3-Py	<i>o</i> -tol	0.38 ± 0.071 (5)	0.54 ± 0.17 (3)	15
10	H	CF ₃	<i>c</i> Pr	5-Pyr	<i>o</i> -tol	0.40 ± 0.070 (4)	1.8 ± 0.34 (4)	37, 33
11	3-F	CF ₃	<i>c</i> Pr	5-Pyr	<i>o</i> -tol	0.37 ± 0.041 (4)	1.2 ± 0.67 (4)	36
(+)-11	3-F	CF ₃	<i>c</i> Pr	5-Pyr	<i>o</i> -tol	0.35	2.5	>30
(-)-11	3-F	CF ₃	<i>c</i> Pr	5-Pyr	<i>o</i> -tol	0.42	2.6	>30
12	4-F	CF ₃	<i>c</i> Pr	5-Pyr	<i>o</i> -tol	0.47 ± 0.11 (3)	*EC _{50.1} ; EC _{50.2} 0.68 ± 0.10; 3.6 ± 1.3 (4)	ND
13	6-F	CF ₃	<i>c</i> Pr	5-Pyr	<i>o</i> -tol	0.47 ± 0.18 (3)	*EC _{50.1} ; EC _{50.2} 0.71 ± 0.13; 4.8 ± 1.3 (4)	ND
14	H	CF ₃	<i>c</i> Pr	<i>c</i> Pr	<i>o</i> -tol	4.8, 4.7	3.2, 4.2	ND
15	H	CF ₃	COCH ₃	5-Pyr	<i>o</i> -tol	15, 15	>30, 21	>30
16	2-F	CF ₃	CH ₃	3-Py	<i>o</i> -tol	1.0 ± 0.14 (3)	2.5 ± 0.26 (3)	ND
17	2-F	CF ₃	CH ₃	3-Py	<i>c</i> Hex	1.7 ± 0.56 (3)	2.6 ± 0.49 (3)	ND
18	H	CF ₃	<i>c</i> Pr	3-Py	<i>c</i> Pr	1.5 ± 0.29 (3)	3.0 ± 0.55 (3)	ND
19	H	CF ₃	<i>c</i> Pr	2Me-3Pyr	<i>c</i> Pr	>30, 14	21, 16	>30
20	H	CF ₃	<i>n</i> Pr	5-Pyr	<i>o</i> -tol	0.31 ± 0.056 (3)	0.52 ± 0.11 (3)	13
21	H	CF ₃	<i>n</i> Pr	3-Py	<i>o</i> -tol	0.23 ± 0.025 (3)	0.41 ± 0.083 (3)	10

^aConcentration response data were collected with technical duplicates or triplicates at each inhibitor concentration. Data were fitted in GraphPad Prism to the inhibitor vs response—variable slope (four parameters) equation to determine the EC₅₀, with the exception of *, where biphasic curves were observed and data were fitted to the biphasic equation with constraints (top = 1.0, bottom >0, and hill coefficients <0) to determine EC_{50.1} and EC_{50.2}. Data are the EC₅₀ mean ± std dev with the number of independent biological replicates shown in parenthesis. Individual values are shown for studies with less than three biological replicates. Ph, phenyl; Py, pyridyl; Pyr, pyrimidinyl; tol, tolyl. Compounds are racemic, unless otherwise indicated.

and 11 [(+)-11 and (-)-11] showed equal potency. Taken together, the data support an absence of enantiomer selectivity for the series.

While the initial hit 3 showed similar activity on both 3D7 and Dd2 parasite lines, a number of subsequent compounds in the series showed reduced activity on Dd2, with differences of up to 5–10-fold observed for the most disparate compounds (e.g., 10, 12, and 13) (Table 1). These differences will be discussed in greater detail below. Cytotoxicity was evaluated using human HepG2 cells. While 3 did not show any activity up to the highest tested concentration of 30 μM, several of the more potent analogues (9, 20, and 21) displayed cytotoxicity with CC₅₀ values in the 10–15 μM range, yielding a selectivity window of 40–50-fold in these cases (Table 1).

Molecular modeling suggested that a *cis*-amide could orient the A, B, and C rings similarly to the tetrazole. A subseries of amides was synthesized to test this hypothesis (22–34) (Table 2). Consistently, 22 and 23 were equipotent to their tetrazole congeners 9 and 10. The NH amides were fivefold less active, as predicted based on conformational considerations (data not

shown). The SAR from the two subseries was found to be similar, consistent with a similar MOA. This includes the finding that for the B-ring, both 3-Py (22, 24, 26, and 28) and 5-Pyr (23, 25, 27, and 29) showed similar activity against 3D7, while similar to the tetrazoles 9 and 10, Dd2 activity on the 5-Pyr tended to be lower than for the 3-Py. The A-ring CF₃ could be replaced with SCF₃ (24 and 25) or OCF₃ (26 and 27), yielding similar potency. The methyl on the C-ring could be extended to ethyl to improve activity approximately twofold (22 vs 28; 23 vs 29), whereas removing the C-ring methyl was associated with an approximately twofold loss in activity (23 vs 30). The addition of a 2-Me to the 5-Pyr at the B-ring led to a substantial 20-fold loss in potency (31 vs 23). As observed with the tetrazole series, the addition of 2-F to the A ring was well tolerated (32 vs 22; compared to 16 in the tetrazole series), while a benzylic cyclopropyl group again improved activity to give 33 (vs 20 and 21 in the tetrazole series), currently our most potent analogue (EC₅₀ = 0.21–0.33 μM on 3D7 and Dd2, respectively). Additionally, as with the tetrazoles, replacement of the C-ring with a saturated ring (piperidine 34) led to a fivefold reduction

Table 2. SAR of the Amide Subseries^a

cmpd	R	R1	R2	R3	B-ring	<i>P. falciparum</i> EC ₅₀ (μM)		cytotox CC ₅₀ (μM) HepG2
						<i>Pf</i> 3D7	<i>Pf</i> Dd2	
22	H	CF ₃	cPr	Me	3-Py	0.34 ± 0.044 (3)	0.59 ± 0.067 (3)	>30
23	H	CF ₃	cPr	Me	5-Pyr	0.40 ± 0.015 (3)	0.79 ± 0.19 (3)	>30
24	H	SCF ₃	cPr	Me	3-Py	0.31 ± 0.078 (3)	0.39 ± 0.045 (3)	>30
25	H	SCF ₃	cPr	Me	5-Pyr	0.26 ± 0.046 (3)	1.0 ± 0.55 (5)	>30
26	H	OCF ₃	cPr	Me	3-Py	0.32 ± 0.035 (3)	0.52 ± 0.055 (3)	>30
27	H	OCF ₃	cPr	Me	5-Pyr	0.24 ± 0.044 (3)	0.59 ± 0.17 (5)	>30
28	H	CF ₃	cPr	Et	3-Py	0.19 ± 0.025 (3)	0.48 ± 0.084 (3)	>20
29	H	CF ₃	cPr	Et	5-Pyr	0.24 ± 0.042 (3)	0.57 ± 0.14 (3)	>25
30	H	CF ₃	cPr	H	5-Pyr	0.72 ± 0.021 (3)	*EC _{50.1} ; EC _{50.2} 2.0 ± 1.4; 16 ± 5.4 (4)	>30
31	H	CF ₃	cPr	Me	2-Me, 5-Pyr	8.1, 7.5	9.8, 7.7	>30
32	F	CF ₃	cPr	Me	3-Py	0.31 ± 0.026 (3)	0.46 ± 0.046 (3)	>30
33	H	CF ₃	nPr	Me	3-Py	0.21 ± 0.021 (3)	0.33 ± 0.035 (3)	>15
34	H	CF ₃	cPr	C**	3-Py	1.8 ± 0.15 (3)	4.2 ± 0.84 (3)	>20

^aConcentration response data were collected with technical triplicates at each inhibitor concentration, and data were fitted in GraphPad Prism to determine the EC₅₀, as described in the Table 1 footnote. Data are the EC₅₀ mean ± std dev with the number of independent biological replicates shown in parenthesis. **C-ring replaced with piperidine.

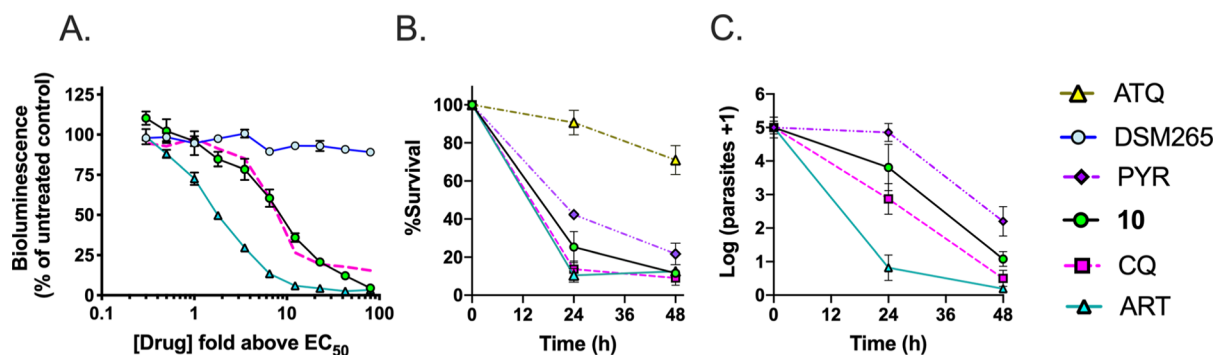


Figure 2. Relative rate of kill of **10** vs control antimalarials. (A) BRRoK rate of kill assay. Conditions used were as described in Figure 1. The mean EC₅₀ for **10** was 0.32 μM, as determined using 72 h SBYR Green assays. DSM265 and ART controls were collected simultaneously to the **10** data. CQ data were replotted from Figure 1 and are provided again in this plot as a reference. (B) Kill rate determination using two-color FACS analysis. Benchmark compounds are described above. Pyrimethamine (PYR) was included as a medium rate of the kill compound. Compounds were plated at 10× EC₅₀, where EC₅₀ values, determined using 48 h hypoxanthine assays, were **10** (1.7 μM), CQ (0.021 μM), ART (0.03 μM), PYR (0.094 μM), and ATQ (0.001 μM). (C) PRR washout assay. Data show % parasite survival vs h of drug treatment prior to drug washout and replating. PYR data were collected simultaneously to **10**. CQ and ART data are historical control data collected in a separate study³⁴ and provided as a reference. Triplicate data were collected at each compound concentration, symbols represent the mean, and error bars represent the std dev.

Table 3. Physicochemical Properties and *In Vitro* Metabolism in Human Liver Microsomes

cmpd	MW	cLog D pH 7.4	predicted pK _a (basic)	CL _{int} (μL/min/mg protein)	kinetic solubility pH 2.0 (μg/mL)	kinetic solubility pH 6.5 (μg/mL)
7	495	5.2	4.6, 3.3	154	12.5–25	1.6–3.1
9	465	5.3	5.1, 2.9	360	12–23	1.5–2.9
10	465	4.6	4.7	261	1.5–2.9	1.5–2.9
22	454	5.3	6.0, 3.4	781	>100	6.3–12.5
23	454	4.6	5.5	531	11–23	>45
32	472	5.4	5.0, 3.4	548	>47	1.5–2.9
34	418	3.9	6.1, 3.4	244	>100	25–50

in activity but showed some promise. Relative to other compounds in the series, compound **30** showed the greatest

loss of potency against Dd2 parasites, requiring over 20-fold higher concentrations for complete killing (Table 2). Cytotox-

icity in the amide series was improved over the tetrazoles, with no compounds showing any cytotoxic activity up to the highest tested concentration of 30 μM (Table 2).

To confirm that the 3-series shows fast kill kinetics, we re-evaluated the kill rate using more potent analogues from both the tetrazole (10) and amide (23) subseries using the BRROK assay cited above. Like 3, both compounds behaved similarly to CQ in this assay, consistent with fast kill kinetics (Figures 2A and S1). Finally, 10 was tested in both a flow cytometry (FACS) assay⁴¹ that detects the ability of parasites to invade new RBCs after incubation with drug and in the PRR-based washout assay,³⁴ with both assays confirming that 10 exhibited kill kinetics similar to CQ, although slower than ART (Figure 2).

ADME Assessment of Selected Tetrazole and Amide Compounds. A preliminary assessment of the physicochemical properties and metabolic stability was conducted for several compounds in the tetrazole and amide subseries (Table 3). Lipophilicity in the series was high, and this property correlated with the overall poor metabolic stability in human liver microsomes for all tested compounds. Compound 7 and some with lower cLog *D* (10 and 34) performed marginally better than other compounds in the series, and overall, the tetrazoles were slightly better than the amides. Solubility in pH 6.5 phosphate buffered saline (PBS) was poor for the tetrazoles but was substantially better for the amides at both pH 2.0 and 6.5, with 34 showing the best overall properties in these assays. Overall, these studies identified a significant metabolic liability that would need to be addressed before these series could be expected to show *in vivo* efficacy.

Life-Cycle Profiling. Representative compounds, one each from the tetrazole (9) and amide (32) series, were profiled against liver- and sexual-stage parasites to determine if the series would have prophylactic or transmission-blocking activity (Table 4). Liver-stage activity was assessed against *Plasmodium*

against a selection of drug-sensitive and drug-resistant parasite lines. Initial work focused on comparing the effectiveness against 3D7 and Dd2 parasites. As noted above, while 3 showed similar activity against these strains (Table 1), a number of analogues in both the tetrazole and amide subseries showed lower activity against Dd2 than 3D7 (Tables 1 and 2). The largest differences (three- to fivefold) were observed for compounds with a 5-Pyr in the B-ring (10, 26), whereas the matched compounds with 3-Py in this position showed smaller (1.4–3.0-fold) effects (9 and 27) based on comparisons of matched pairs that contained only variations in this position (Figures 3 and S2). Additionally, for several analogues (12, 13, and 30) containing the 5-Pyr in the B-ring, we observed biphasic concentration response curves versus Dd2. In these cases, up to a 20-fold potency difference was observed between 3D7 and the second of the fitted EC_{50} values determined for Dd2, whereas the more potent EC_{50} values were similar to that observed for 3D7 (Figure 4 and Tables 1 and 2). These data suggest that a second target might be responsible for the reduced Dd2 efficacy at higher concentrations for these compounds. In contrast, biphasic concentration response curves were never observed versus 3D7 for any compound. Encouragingly, our data show that it is possible to identify compounds with similar potency against 3D7 and Dd2, for example, by avoiding the 5-Pyr that frequently led to biphasic concentration response curves. These results highlight the value of including multiple parasite lines in early-stage compound evaluation.

To further probe the MOA, 9 and 10 were evaluated against two panels of resistant parasite lines that were either obtained as clinical isolates⁴² or were generated in Dd2 parasites through *in vitro* selections with various antimalarials. Data were compared to the drug-sensitive 3D7 and NF54 strains (Table 5; note that 3D7 is a clone of NF54). No cross resistance was observed for 9 across the two panels. In contrast, 10 showed reduced potency against the CQ-resistant Dd2 and piperaquine (PPQ)-resistant RF12 strains, although reduced activity was not observed against other tested lines with other drug-resistant phenotypes. Interestingly, both 9 and 10 were more effective against 7G8 parasites than any of the other tested lines, even though this line, similar to Dd2, RF12, K1, and TM90C2B, contains point mutations in the *P. falciparum* CQ resistance transporter (*PfCRT*; Table 6).

PfCRT in certain mutant forms mediates CQ efflux from the DV and is causal for CQ resistance.^{23,43–45} While each strain harbors a key set of *PfCRT* mutations (including K76T, Table 6) that confer CQ resistance, the specific set of point mutations differs across strains and mediates differences in sensitivity to CQ and other 4-aminoquinolines such as PPQ and amodiaquine.^{44,46,47} The 7G8 mutational background has also been reported to increase sensitivity to lumefantrine (LUM).^{46,47} Thus, each *PfCRT* isoform could display different binding affinities and transport levels of 3-series compounds as well and thus modulate parasite susceptibility to these compounds differentially. This hypothesis was investigated by testing gene-edited isogenic lines that allow comparison between different *pfcr*t alleles with varied sensitivity to CQ in the same genetic background. These lines were generated previously by zinc-finger nuclease-mediated editing of Dd2 parasites to insert (1) the wild-type *pfcr*t allele (Dd2-GC03); (2) the recombinant Dd2 *pfcr*t allele (Dd2-Dd2) (differing from wild-type *PfCRT* by eight point mutations Table 6); or (3) the recombinant Dd2 *pfcr*t allele and the M343L mutation (Dd2-M343L), resulting in PPQ resistance.^{44,46–49} We found that either the Dd2 *PfCRT*

Table 4. Life Cycle Profiling^a

cmpd	<i>Pb</i> liver-stage EC_{50} (μM)	HepG2 CC ₅₀ (μM)	DGFA (male/female) gametocytes EC_{50} (μM)
9	7.3, 12	19, >17	>25/>25
32	7.0, 16	24, 24	~60% at 25 μM />25

^a EC_{50} values are shown for two independent replicates. DGFA, dual gamete formation assay.

berghei to determine whether compounds could block liver-stage development in HepG2 cells infected by sporozoites.^{19,21} Modest activity was observed in this assay, but the *Pb* liver-stage EC_{50} for both compounds was 20- to 30-fold higher than for *P. falciparum* blood stages. The dual gamete formation assay (DGFA) was used to assess the ability of compounds to block maturation of both male and female stage V gametocytes, providing a readout of functional viability. The assay identifies compounds that either kill stage V gametocytes or interfere with gamete formation. No activity was observed against female gametocytes for either compound, while modest activity was seen for 32 against male gametocytes (~60% inhibition at 25 μM). Thus, the 3-series compounds do not have significant liver-stage or transmission-blocking activity, positioning them for use solely for treatment of ABS infections.

Evaluation of Cross Resistance to the Known Drugs Suggests a Common Resistance Mechanism with H₂-Inhibiting Antimalarials. To obtain insight into the potential MOA of the 3-series compounds, we evaluated compounds

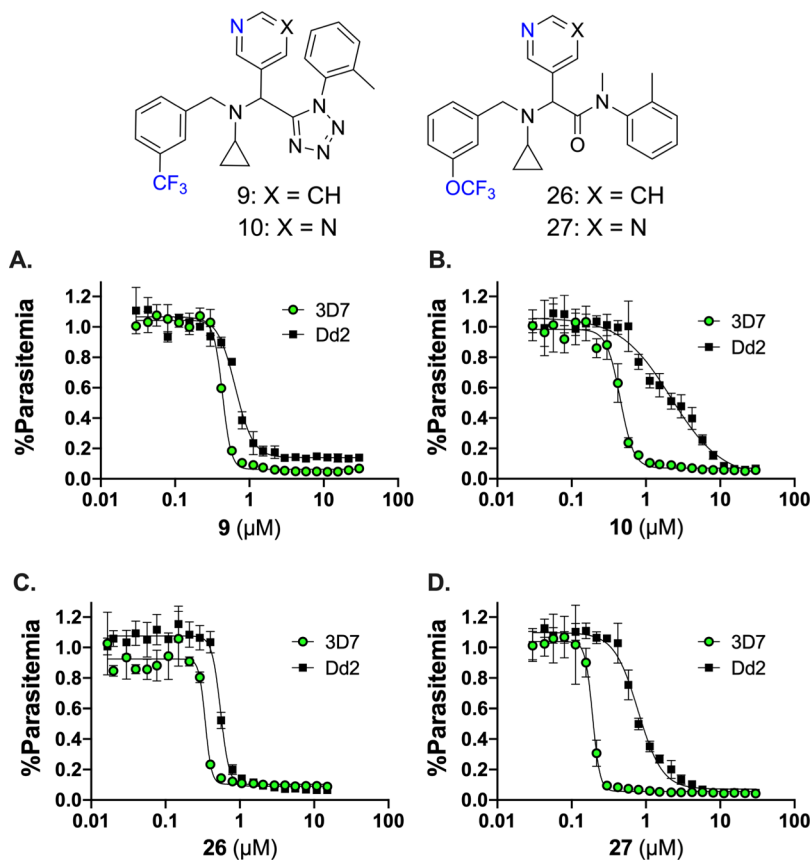


Figure 3. Reduced efficacy of 3-analogues containing 5-Pyr against *P. falciparum* Dd2 compared to 3D7 parasites. Comparison of representative concentration response curves for tetrazoles **9** (A) and **10** (B) and for amides **26** (C) and **27** (D), tested against 3D7 (green circles) and Dd2 (black squares) parasites. Results showed that compounds containing 5-Pyr have poorer activity against Dd2 than do compounds containing 3-Py in the B-ring. Compound structures are shown above the graphs. Data were fitted to the $[I]$ vs response, variable slope (four parameter) equation in GraphPad Prism to determine the EC_{50} . Triplicate data were collected at each concentration, symbols represent the mean, and error bars represent the std dev. EC_{50} data are reported in Tables 1 and 2, which contain average data for at least three biological replicates.

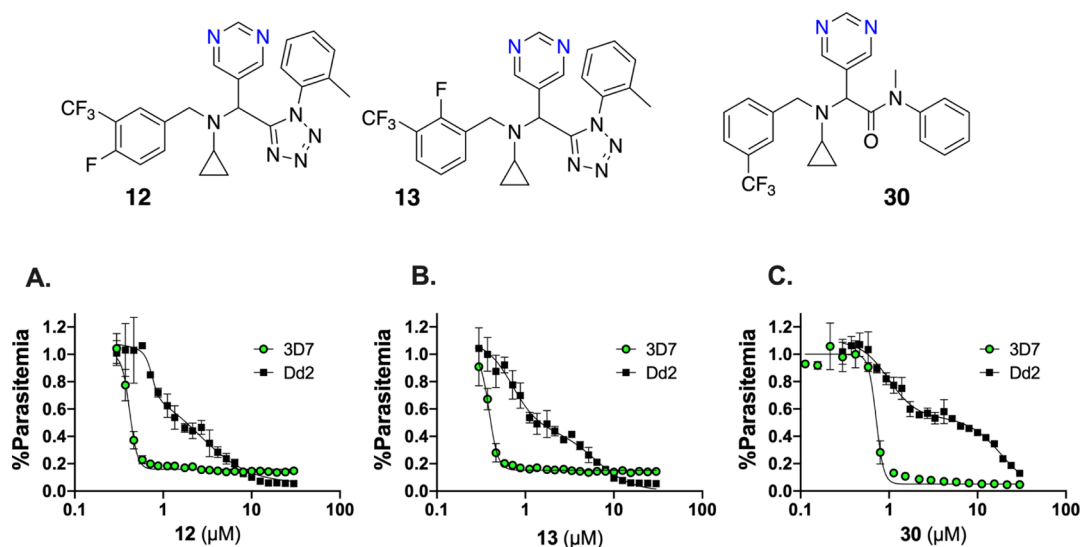


Figure 4. Biphasic growth curves were observed for select 5-Pyr 3-series compounds assayed against Dd2 parasites. Comparison of representative concentration response curves for tetrazoles **12** (A) and **13** (B) and for amide **30** (C) tested against 3D7 (green circles) and Dd2 (black squares) parasites. Compound structures are displayed above the graphs. Triplicate data were collected at each concentration, symbols represent the mean, and error bars represent the std dev. EC_{50} data and curve fitting methods are reported in Tables 1 and 2.

background or the Dd2-M343L background led to a two- to threefold increased sensitivity to both **9** and **10** (Table 5) relative to Dd2-GC03. These data suggest that the wild-type

PfCRT transporter might bind better to **9** and **10** than do the variant Dd2 or Dd2 + M343L isoforms, leading to lower drug concentrations in the DV. Interestingly, the addition of M343L

Table 5. Activity of 9 and 10 Versus Parasite Strains with Resistance to Compounds from Diverse Structural Classes and Mechanisms of Action

<i>Pf</i> parasite line	resistance profile	9	9	10	10
		EC ₅₀ (μM)	fold diff ^a	EC ₅₀ (μM)	fold diff ^a
Drug-Resistant Field Isolates ^{42,44,49}					
3D7	sensitive	0.38	1.0	0.40	1.0
NF54	sensitive	0.48	1.3	0.83	2.1
K1	CQ, PYR	0.36	0.95	0.46	1.2
7G8	CQ, PYR	0.18 ± 0.042 (3)	0.47	0.16 ±0.024 (3)	0.40
TM90C2B	CQ, ATQ, PYR	0.46	1.2	0.66	1.7
RF12	PPQ, PYR	0.61	1.6	1.1	2.8
Dd2	CQ, PYR	0.54	1.4	1.8	4.5
<i>Pf</i> CRT Gene Edited Isogenic Lines					
Dd2-GC03	sensitive	0.89 ± 0.12 (3)	1.0	4.8	1.0
Dd2-Dd2	CQ	0.45 ± 0.13 (3)	0.53	2.4	0.50
Dd2-M343L	PPQ, CQ	0.38 ± 0.10 (3)	0.41	0.90	0.19
Lab-Derived Dd2 Lines Resistant to Development Candidates					
PfeEF2	DDD107498 ⁸⁵	0.92	1.7	1.6	0.89
Pfpi4K	MMV390048 ¹⁸	0.75	1.4	2.0	1.1
PfDHODH	DSM265 ²⁵	0.80	1.5	2.0	1.1
Pfcarl	KAF156 ⁸⁶	0.65	1.2	2.0	1.1
PfCytB	ELQ300 ⁸⁷	0.85	1.6	2.0	1.1

^aFold differences were calculated relative to 3D7 for field isolates, relative to Dd2-GC03 for the isogenic gene-edited lines, or relative to Dd2 for lab-selected Dd2 resistant lines. The GC03 line (which contains the *pfcr* wild-type allele, also found in 3D7 or NF54) was previously isolated from the Dd2 × HB3 cross and is CQ-sensitive. The gene-edited lines were constructed using customized zinc-finger nucleases and have been previously reported.^{46–48} Dd2-GC03 was derived by introducing the 3D7 *pfcr* sequence into Dd2 in place of the endogenous *pfcr* Dd2 locus (sequence shown in Table 6). Dd2-Dd2 was engineered using the same method to replace the endogenous *pfcr* locus with the recombinant Dd2 sequence, and Dd2-M343L replaced the endogenous *pfcr* locus with the recombinant Dd2 sequence and the PPQ resistance-conferring M343L^{44,49} mutation. Concentration response data were collected with technical duplicates at each inhibitor concentration, and reported data represent the average of two biological replicates, and where additional biological replicates were collected (number in parenthesis), the std dev is provided. Additional replicate data for NF54 can be found in Table S2A. Development candidates used for selections are listed, and parasite lines are named based on the protein target of the resistance allele. CQ, chloroquine, ATQ, atovaquone, PYR, pyrimethamine, and PPQ, piperaquine. Data for Dd2 and 3D7 were taken from Table 1.

Table 6. Documented Point Mutations in *Pf*CRT Across the Tested Strains^a

Strain	PfCRT position and encoded amino acid										
	72	74	75	76	97	220	271	326	343	356	371
3D7	C	M	N	K	H	A	Q	N	M	I	R
NF54	C	M	N	K	H	A	Q	N	M	I	R
Dd2	C	I	E	T	H	S	E	S	M	T	I
7G8	S	M	N	T	H	S	Q	D	M	L	R
RF12	C	I	E	T	Y	S	E	S	M	T	I
K1	C	I	E	T	H	S	E	S	M	I	I
TM90C2B	C	I	E	T	H	S	E	S	M	T	I

^aData were taken from refs 23, 43, 44, 49, and 88. Colors highlight residue differences between strains: yellow (3D7 and Dd2), green (3D7 and 7G8), and turquoise (3D7 and RF12). RF12 is also known in the literature as PH1263-C. 3D7 is a clone of NF54.⁴⁹

has also been reported to reduce the degree of CQ-resistance by two- to threefold, compared with the Dd2 isoforms.⁴⁹ The finding that the EC₅₀ for 10 on Dd2-GC03 is higher than for the Dd2-Dd2 line shows that the poor activity of 10 on Dd2 relative to 3D7 is not linked to differences in the *pfcr* allele.

Heme Polymerization is Inhibited by 3-Series Compounds. Similarities between CQ and the 3-series compounds suggested to us the potential for a common MOA. CQ functions by interrupting heme detoxification via inhibition of the biomineralization of toxic labile heme into the chemically inert Hz in the DV.^{43,50,51} Similarities include the killing kinetics, the life-cycle profile showing activity only on ABS, and the observations that CQ-resistant (7G8 and Dd2) and genetically engineered lines containing *Pf*CRT mutations showed differ-

ential sensitivity to compounds in the 3-series, suggesting that like CQ and other quinolines, the 3-series compounds targeted a process in the DV. Additionally, the lack of enantiomer selectivity of the 3-series supports the hypothesis of a nonprotein target such as heme polymerization.

To investigate the activity of 3, 9, and 10 against the heme detoxification pathway, we tested the ability of these compounds to inhibit conversion of hematin (Fe(III)PPIX) to the synthetic β-hematin (βH) form of Hz. These experiments used a pyridine-based detergent-mediated colorimetric assay that simulates the physiological microenvironment of the DV.⁴⁷ Standard antimalarials with diverse MOAs were tested in parallel to serve as controls. As expected, CQ, amodiaquine, MFQ, and pyronaridine inhibited βH formation with IC₅₀ ≤ 100 μM, while pyrimethamine, dihydroartemisinin, and doxycycline did not inhibit conversion of hematin to βH (Figure 5). Among the tested compounds, 9 inhibited βH formation with the same potency as MFQ, while 10 showed weaker inhibition. Compound 3 was nearly inactive in the concentration range that could be studied (Figure 5). The IC₅₀ values for inhibition of βH formation (Figure 5) of the 3-series compounds correlated loosely with their EC₅₀ values for inhibiting NF54 proliferation (Tables 5 and S2). 9 was the most potent in both assays, supporting the hypothesis that the mechanism of cell killing was related to inhibition of βH formation. The concentration of the compound required to inhibit βH formation was ~1000-fold higher than the EC₅₀ for parasite survival not only for the 3-series but also for the 4-aminoquinolines. These differences are thought to reflect the

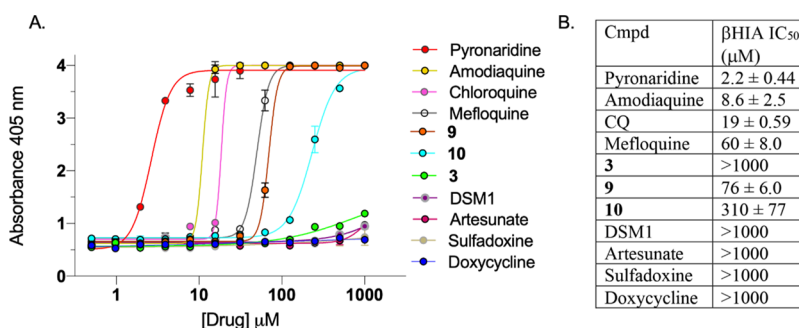


Figure 5. β -Hematin inhibition assay (β HIA) for 3-series compounds in comparison to antimalarial control compounds. (A) Representative titration data showing inhibition of β -hematin formation vs concentration profiles for 3, 9, and 10 in comparison to known antimalarials, using the β -hematin inhibition assay (β HIA).⁸⁹ Positive (pyronaridine, amodiaquine, CQ, and MFQ) and negative controls were assayed, with the latter representing a diverse set of MOAs (the DHODH inhibitor DSM1,⁹⁰ artesunate, sulfadoxine, and doxycycline). Data show the mean \pm std dev for duplicate data at each compound concentration. Data were fitted to the sigmoidal concentration response (variable slope) equation in GraphPad Prism to determine the IC₅₀. (B) Fitted IC₅₀ values. Data represent the mean \pm std dev for four independent studies.

fact that drug accumulation in the DV is in a function of pH trapping;⁵² hence, the extent of accumulation determines the concentration at the site of action.

Cellular Heme Fractionation. To mechanistically validate the *in vitro* heme polymerization results described above, we applied a heme fractionation assay to measure inhibition of Hz formation in NF54 parasites. In this assay, “% free heme”, % Hz (determined as proportions of total heme species extracted), and levels of “free” heme-Fe and Hz-Fe (absolute amounts of each species per cell calculated from the total amount of Fe obtained using a heme standard curve) were quantified from isolated trophozoites after their treatment with compounds. This assay tested a range of compound concentrations at or above their EC₅₀ for antimalarial activity (0.5 \times to 3 \times EC₅₀). For the positive CQ control, both the % “free” heme and the levels of “free” heme-Fe showed a significant concentration-dependent increase as the drug concentration was increased above the EC₅₀ compared to the no-drug control (Figure 6A(i)), whereas Hz and Hz-Fe decreased over the same concentration range (Figure 6A(ii)). Overlaying the parasite survival curve with the “free” heme-Fe titration curve showed that the concentration of CQ leading to 50% activity (EC₅₀ for heme-Fe release vs EC₅₀ for parasite survival) was similar in both assays (Figure 6A(iii)), consistent with CQ being a bona fide inhibitor of Hz formation.⁵³ This result contrasts with the data for the dihydrofolate reductase inhibitor pyrimethamine (Figure 6B), included as a negative control to illustrate the robustness of this protocol in discriminating agents that do not inhibit Hz formation. No significant increase in free heme was observed over the course of the titration, regardless of drug concentration.

Treatment with 9 and 10 led to a robust buildup of free heme (calculated as a percent of total heme species) and the level of heme-Fe, with a corresponding decrease in Hz levels (Figure 6C,D). These compounds led to significantly larger amounts of free heme release (sixfold increase in free heme-Fe for 9 and 10 vs only twofold for CQ) and a corresponding reduction in Hz levels at 3 \times EC₅₀ compared to CQ (2-fold decrease in Hz heme-Fe for 9 and 10 compared to 1.3-fold for CQ), demonstrating a higher amount of free heme at the compound concentrations that disrupt parasite growth. Similar to CQ, overlaying the parasite survival curve with the “free” heme-Fe titration curve showed that the concentrations of 9 and 10 at the EC₅₀ of heme-Fe release versus EC₅₀ for parasite survival were very similar in both assays. These data suggest that the MOA of the 3-series compounds is at least in part due to inhibition of Hz formation.

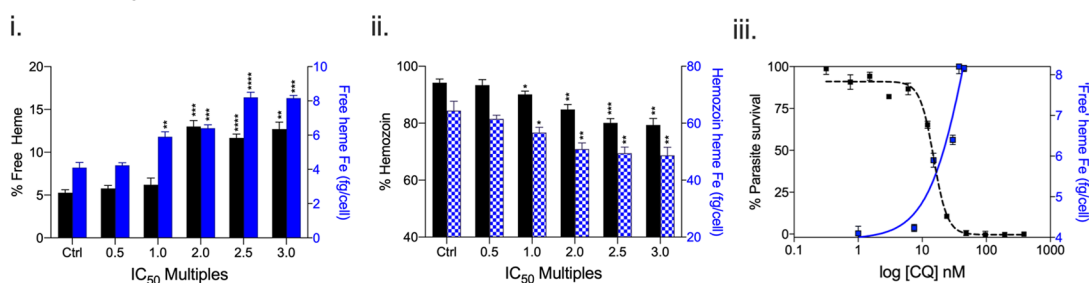
Selections for *P. falciparum* 3D7 Parasites Resistant to Compound 9.

To obtain additional insight into the potential mode of resistance to 3-series compounds, we performed single-step selection studies to obtain parasites resistant to 9. Selections were performed with a starting parasite inocula of 2×10^9 3D7 parasites per flask, and two separate flasks were pressured with 9 at a concentration of 3 \times EC₅₀. Drug-treated parasites cleared in both flasks by day 5 and recrudescence on day 25. Bulk cultures showed EC₅₀ shifts of only 2.4- to 3.4-fold compared to the parental line. Three clones were then obtained from each flask by limiting dilution. EC₅₀ and ED₉₀ shifts for these six clones were found to be a modest 2.8–2.6-fold (Table 7). The high starting inocula and the modest shifts in EC₅₀ for the selected mutant lines suggest that it is relatively difficult to evolve resistance against 9.

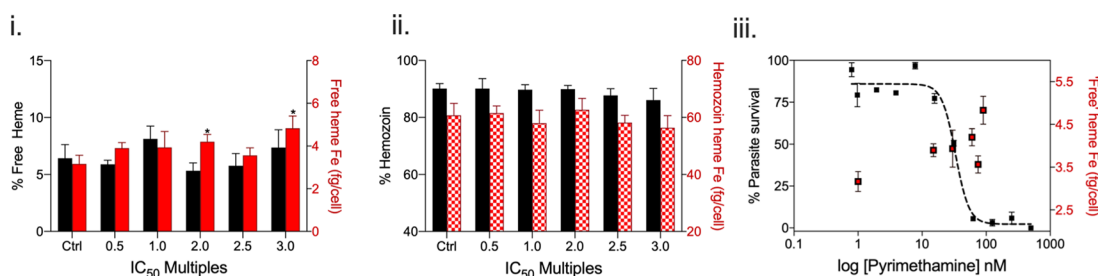
WGS performed on two clones per flask found that each clone had a copy number variation (CNV) on chromosome 5, with flask 1 (F1) clones showing three- to fourfold amplification and flask 2 (F2) clones showing fivefold amplification of the region (Tables S4 and S5 and Figure S3A). Clones from the two flasks differed in the chromosome 5 segment that was amplified. Nonetheless, all clones overlapped in the multidrug resistance gene 1 (*pfmdr1*, PF3D7_0523000) locus. This gene has previously been shown to be involved in MFQ, LUM, and quinine drug resistance and can also modulate CQ potency.^{54,55} This was the only change observed in all four clones, suggesting that it represents the major mechanism of resistance to 9 in these lines.

In addition to the CNV on chromosome 5, F2 clones A10 and A11 had another set of CNVs on chromosome 12, showing an approximately twofold amplification (Table S5 and Figure S3B). It is interesting to note that one of the eight genes in this amplified locus (PF3D7_1223700) encodes a proposed vacuolar iron transporter, which could potentially be involved in modulating the consequences of disrupting heme polymerization in the DV. Finally, F1 clones F1-B6 and F1-E4 had single nucleotide polymorphisms (SNPs) in two common genes (Table S6), an M199I-substitution in PF3D7_0208200 (KRR1 small subunit processome component) and a N353K-substitution in PF3D7_1316700 (unknown function), while F1-B6 also contained a D4190N mutation in PF3D7_1343800 (unknown function). The relevance of these SNPs to the resistance mechanism of 9 is unknown.

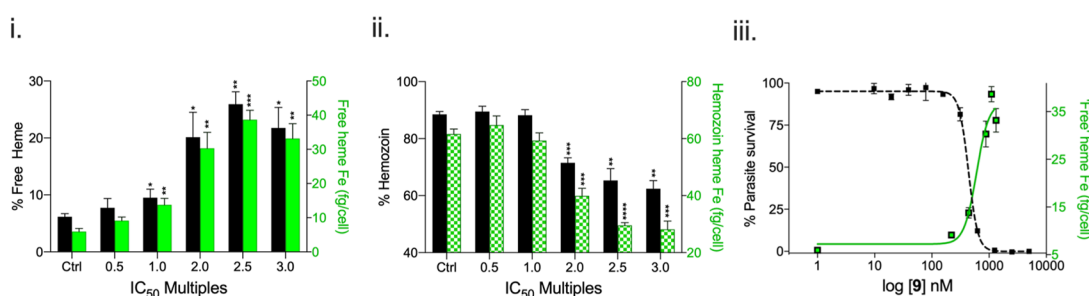
A. Chloroquine



B. Pyrimethamine



C. 9



D. 10

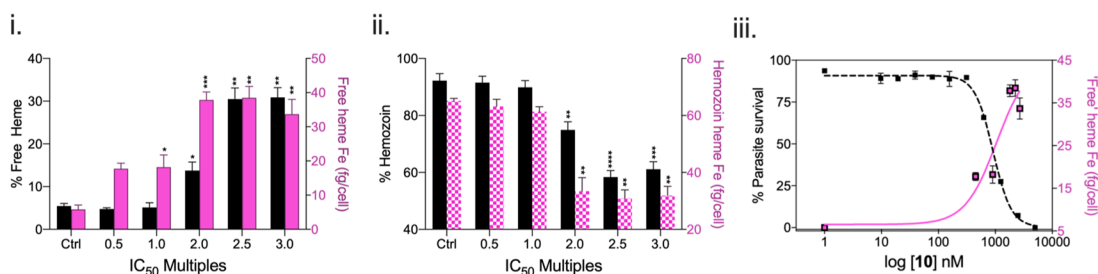


Figure 6. Cellular heme fractionation and concentration response versus parasite survival. Data are shown for (A) CQ, the positive control, for (B) PYR, the negative control, and for two 3-analogues, (C) compound 9 and (D) compound 10. Panels (i,ii) Heme species present as “free” heme (panel i) and Hz Fe (fg) (panel ii) isolated per cell from drug-treated *PfNFS4* parasites. Data represent the mean \pm std dev from three biological replicates, each arising from two technical replicates (see Table S3). Panel (iii) Overlay of parasite survival with the total amount of “free” heme-Fe as a function of drug concentration. Free heme data represent the mean \pm std dev from three biological replicates (taken from panels i), while representative parasite survival data from one biological replicate with technical duplicates is displayed (see Table S2A for average EC₅₀'s from three biological replicates). Data were fitted to the sigmoidal concentration response (variable slope) equation in GraphPad Prism. Calculated EC₅₀ values for the drug concentration giving 50% response are as follows: CQ, 58 nM (heme) and 15 nM (survival); PYR, >100 nM (heme) and 33 nM (survival); cmpd 9, 620 nM (heme) and 440 nM (survival); and cmpd 10, 1040 nM (heme) and 910 nM (survival). See Table S2A,B for error analysis. Significance was assessed using a two-tailed Welch's *t*-test, where * <0.05, ** <0.01, and *** <0.001.

DISCUSSION

The ability of *P. falciparum* to develop resistance to virtually every drug that has been used clinically exemplifies the importance of working on this pathogen to further elucidate its biology and identify new drugs. Herein, we describe the identification of a novel, fast-acting antimalarial compound series that has efficacy against ABS parasites. In addition to

showing fast kill kinetics, selection of resistant parasites toward one of the more potent compounds 9 generated only modest levels of resistance (two- to threefold) and WGS suggested that resistance was associated with amplification of the *pfmdr1* gene. We showed that 3-series compounds 9 and 10 inhibited heme polymerization both *in vitro* and in *P. falciparum* cellular assays. Importantly, 9 showed equal efficacy on both CQ-sensitive and

Table 7. *In Vitro* Selections for Pf3D7 Parasites Resistant to 9 Showing EC₅₀/EC₉₀ Shifts of Clonal Lines^a

clone	parental	9 resistant clonal 3D7 lines					
	3D7-A10	F1-B6	F1-C1	F1-E4	F2-A10	F2-A11	F2-H12
EC ₅₀ μ M	0.30 \pm 0.033	0.55 \pm 0.058	0.54 \pm 0.061	0.74 \pm 0.12	0.83 \pm 0.11	0.67 \pm 0.029	0.64 \pm 0.055
fold shift	NA	1.8	1.8	2.5	2.8	2.3	2.2
EC ₉₀ μ M	0.59 \pm 0.12	1.1 \pm 0.16	1.0 \pm 0.17	1.5 \pm 0.21	1.5 \pm 0.10	1.3 \pm 0.041	1.3 \pm 0.078
fold shift	NA	1.9	1.8	2.6	2.6	2.3	2.2

^aData represent the mean \pm standard error of the mean for three independent replicates.

CQ-resistant strains. Thus, the 3-series meets the objective of identifying fast kill compounds with a relatively low propensity of resistance for the treatment of malaria, and they provide a new scaffold that targets heme polymerization, a highly successful strategy for killing malaria parasites. Based on their lack of liver-stage or sexual-stage activity, these compounds would be best positioned in the portfolio for treatment, and their fast kill kinetics could allow them to be suitable for development in non-ART-based therapies. Further work to optimize both potency and drug-like properties would however be needed for this series to advance to lead optimization and to *in vivo* activity.

A limited medicinal chemistry effort was undertaken for the 3-series to define the structural requirements for activity. We found that parasite killing was not dependent on the stereochemistry and that both enantiomers were equally active for those that were tested. The A- and B-rings could be aryl or heteroaryl, but they could not be removed or replaced with aliphatic rings. Substantial substitution on the A ring was tolerated, which allowed us to replace the original Br/OMe substitution with more drug-like CF₃/F groups. Similarly, we were able to improve the polarity of the series by replacing the B-ring phenyl group with heteroaryl rings including 3-pyridine (3-Py) and 5-pyrimidine (5-Pyr). This ring showed the steepest SAR profile with substantial loss in activity associated with substitution on various positions or alternative heteroaryl rings. Activity was improved by replacing the *N*-methyl group with larger *N*-alkyl groups, and the benzylic CH₂ could be replaced with a cyclopropyl group, blocking a potential metabolic liability. The tetrazole could be replaced with a conformationally restricted amide bond, and both series showed similar SAR. Overall, potency improvements of 10–20-fold were obtained relative to the initial hit 3. The amide subseries generally showed better selectivity than the tetrazoles. Lipophilicity, indexed by Log *D*, was high throughout both subseries and metabolic stability was generally poor, although we were able to make some improvements in aqueous solubility.

Profiling of a panel of drug-sensitive or -resistant strains provided the first insights that the 3-series might share a common MOA with Hz inhibitors such as CQ. Direct biochemical evidence that the 3-series compounds inhibit heme polymerization was obtained both *in vitro* and in cell-based assays. We showed that 9 and 10 inhibited heme biomineralization in the *in vitro* β H inhibition assay, while in the cell-based assay, treatment with these compounds caused a CQ-like signature of an accumulation of free heme with commensurate decreases in Hz levels. These effects titrated with the same dose response as parasite killing. Taken together, these data strongly implicate inhibition of Hz formation as one, but perhaps not the sole, MOA of this series. Interestingly, the levels of free heme generated in the presence of 9 and 10 are three- to fourfold higher than those observed for CQ across the dose response range, with the larger differences observed at higher drug concentrations. These results could reflect divergent

interactions of the two compound classes with heme molecules during heme–drug complex formation. Indeed atomic-force microscopy studies have shown that the various antimalarial 4-aminoquinolines affect the biomineralization of heme molecules in different ways, with CQ and quinine providing the most efficient blocking by forming interactions across the flat surface face (“step-pinning”), whereas MFQ and amodiaquine block the addition of heme only to the step edge (“kink-blocking”).⁵¹

Resistance selection studies uncovered resistance mechanisms that overlapped with the CQ-related quinolines such as MFQ, providing an additional link between the 3-series and quinoline compounds. First, we observed that the 3-series has a relatively low propensity to develop resistance as selections with 10⁹ parasites yielded EC₅₀ shifts of only two- to threefold. Our WGS analysis found that the one genetic change common to all the resistant clones was three- to fivefold amplification of the *pfmdr1* gene, which encodes the *P*-glycoprotein transporter Pgp1. *pfmdr1* amplification is a major driver of clinical and parasite *in vitro* resistance to MFQ.^{55,56} The level of resistance observed for 9 was less than that reported for MFQ selection studies, where a lower level of amplification of the *pfmdr1* locus (twofold) yielded a fivefold IC₅₀ increase and which could be selected with a lower starting inocula (\sim 10⁸ parasites).⁵⁷ A greater impact of amplification was also reported for dihydroorotate dehydrogenase (DHODH) inhibitors, where threefold amplification of the *dhodh* locus led to a fivefold EC₅₀ increase from \sim 10⁷ parasites⁵⁸ and five- to sixfold amplification arising from \sim 10⁸ parasites led to a sevenfold EC₅₀ increase.²⁵ Additionally, for DHODH inhibitors, multiple SNPs resulting in >10 to 30-fold shifts in EC₅₀ have been identified at a frequency of \sim 10⁸ parasites.^{25,59} Similar findings have also been reported for other antimalarials in preclinical development where minimum inoculum of resistance of 10⁶ to 10⁸ parasites, mediated often by SNPs or CNVs, led to resistance levels that can range from 2- up to 1000-fold based on the target, the genetic change, and the compound (e.g., PfATP4 or eEF2 inhibited by SNPs in KAE609 or DDD107498, respectively⁴). In this light, our finding of low-level resistance mediated by *pfmdr1* amplification is a favorable feature of the 3-series.

The interplay between PfMDR1 and PfCRT and the impact of their allelic variation on drug resistance are complex and compound-dependent. While CQ resistance is primarily associated with PfCRT mutations,^{23,43–45} low-grade resistance to other quinolines such as MFQ and the arylaminoalcohol LUM is associated with PfMDR1 genetic changes (amplifications or point mutations).^{46,47,60} PfCRT is localized to the DV membrane and transports compounds out of the DV. PfMDR1 also appears to be primarily localized to the Plasmodium DV membrane of the trophozoite,⁶¹ where it has been associated with solute uptake into the vacuole.^{55,60,62} Low-level expression of PfMDR1 at the plasma membrane has also been reported,⁶¹ leaving open the possibility that it could be involved in efflux of compounds out of the parasitized red cell, similar to its

mechanism of resistance in mammalian cells. Within this complex milieu, the potency of any given compound is dependent on the concentrations that can reach the DV, which could be influenced by binding affinity to the parasite line-specific transporter isoforms of *PfCRT* and *PfMDR1* and by nonreceptor-mediated partitioning between the various cellular compartments related to the physical properties of the compound. Our studies on the 3-series suggests that like MFQ and LUM, their efficacy can also be modulated by both transporters but to a lesser extent than for the quinolines. Analysis of the gene-edited lines showed that **9** and **10** were more potent on lines harboring *PfCRT* mutations that are observed in CQ-resistant parasites than on parasites expressing the wild-type allele. These data provide direct evidence that the *pfcr1* allele impacts the potency of 3-series compounds and suggest that the wild-type isoform might bind to and transport these compounds better than isoforms found in CQ-resistant parasites. This result is similar to earlier reports for LUM.⁴⁷ Importantly, these data provide evidence that the 3-series will be fully effective against CQ-resistant parasites harboring *PfCRT* mutations found in malaria-endemic regions.

An identified exception to the promising activity on CQ-resistant strains was identified for 3-series analogues that contained 5-Pyr in the B-ring (e.g., **10**). These tended to show poorer activity against Dd2, while still being effective against 3D7 and 7G8. Some analogues also exhibited biphasic concentration response curves versus Dd2 parasites. The Dd2 line has a separate *PfCRT* isoform compared to the 7G8 line^{43,44} for which higher potency for both **9** and **10** was observed, but data on the gene-edited lines that harbored only the *PfCRT* changes associated with Dd2 suggested that the poor activity of **10** on Dd2 is unrelated to *PfCRT*. *PfMDR1* SNPs might also impact the potency in these cases. Dd2 encodes the N86Y mutation, whereas 7G8 carries the S1034C/N1042D/D1246Y haplotype. Both *PfMDR1* isoforms sensitize parasites to MFQ and LUM (when expressed in parasites with a single copy of *pfmdr1*) and impact multiple antimalarials that engage with the heme degradation pathway, either by causing increased sensitivity or by mediating a degree of resistance.^{60,63,64} These data suggest that the N86Y mutation could be associated with the poor activity of some 3-series analogues against Dd2 and could support a model whereby the N86Y *PfMDR1* mutation leads to reduced levels of 5-Pyr analogues such as **10** in the DV, while not impacting localization of the 3-Py analogues such as **9**. The interplay between the two transporters might also contribute to the biphasic curves observed with the 5-Pyr 3-series analogues (e.g., **10**). Dd2 parasites also express 2 to 3 copies of *pfmdr1*, contrasting with the single copy of *pfmdr1* expressed by 3D7 and 7G8 parasites, which may further contribute to the observed differences between Dd2 and other parasite lines. These differences in potency provide a path forward for future medicinal chemistry as compounds with 5-Pyr in the B-ring would be disfavored going forward.

An open question that remains is how the 3-series analogues interact with heme. The crystal structure of halofantrine–ferriprotoporphyrin IX shows that the basic amine of halofantrine (related to quinine) interacts with a carboxylate from heme, while the hydroxyl coordinates to the heme iron.⁶⁵ Indeed, a characteristic of nearly all heme-interacting antimalarials is the presence of a protonatable amine. These groups appear to be important for interaction with heme and for accumulation in the low pH environment of the DV. All of the 3-series compounds with $EC_{50} < 1 \mu M$ have predicted pK_a values

within reasonable physiological pH ranges, with the central tertiary nitrogen present in all molecules and calculated pK_a values around 5–6, suggesting that 3-series compounds may also interact with heme through this basic amine (Table 3). For example, the acetamide **15** lacks a basic amine and is essentially inactive. Similar to the crystal structure of halofantrine, the structure of MFQ bound to ferriprotoporphyrin IX shows an alkoxide bound to Fe and a salt bridge between a basic amine and the porphyrin carboxylate.⁶⁶ In this context, we note that the amine-tetrazole or amine-amide distance in the 3-series is similar to the amine-alcohol distance in MFQ. This observation prompts the speculation that the tetrazole or amide might bind Fe, while orienting the basic amine in a position to interact with the heme carboxylate.^{67,68}

CONCLUSIONS

Herein, we have described a novel tetrazole-based series with antimalarial activity against ABS parasites. The compound class exhibits a fast kill rate and a relatively low propensity to develop resistance, both desirable properties for new antimalarial drugs. The MOA of the series appears to be inhibition of heme polymerization in the parasite DV, similar to 4-aminoquinolines such as CQ. The series thus provides a new chemical scaffold that functions at least in part by this highly effective mechanism for killing malaria parasites. Novel compounds that function by blocking heme biomineralization have been sought through secondary screening of HTS hits from phenotypic ABS screens, and while some new chemical entities that target this mechanism have been discovered, none have yet progressed to preclinical development.^{50,69,70} Our initial SAR exploration has revealed areas of the scaffold that are subject to modification to optimize activity and physicochemical properties and has shown that substantial improvements are possible. Further efforts will be required to identify compounds with improved potency and ADME properties that will support *in vivo* efficacy and eventual development. The 3-series also provides new tools for studying the heme biomineralization mechanism and the impact of inhibiting this process on the parasite.

EXPERIMENTAL SECTION

Human Samples. Human biological samples were sourced ethically, and their research use was in accordance with the terms of the informed consents under approved IRB/EC protocols for each site.

***P. falciparum* Culture.** *P. falciparum* cultures were maintained at 2% hematocrit using human blood type O+ RBCs (Valley Biomedical) employing a culturing method adapted from Trager and Jensen.⁷¹ Culture media contained the RPMI 1640 medium (Gibco) + 25 mM HEPES and 0.5% Albumax-I, supplemented with 23 mM sodium bicarbonate and 92 μM σ -hypoxanthine.

Determination of Compound Potency against *P. falciparum* In Vitro. Antiplasmodial activity was evaluated using a parasite growth SYBR Green-based inhibition assay adapted from published methods.^{26,27} For the primary screen (plated at 5 μM) and for hit validation three-point cherry pick concentration response curves (plated at 5, 1.7, and 0.42 μM), we acoustically dispensed compounds [30 nL of 5 mM stocks in dimethyl sulfoxide (DMSO)] into wells using a Labcyte-Echo-555 dispenser. Concentration response curves on repurchased or synthesized compounds were generated from serial dilutions prepared in DMSO in triplicate and plated using a Tecan D300e digital dispenser. The DHODH inhibitor DSM265²⁵ served as a positive control, and 0.5% DMSO was plated as a negative control, with all wells normalized to a final concentration of 0.5% DMSO. Culture suspensions were prepared to a 0.5% starting parasitemia at 2% hematocrit and were dispensed (60 μL) using a BioTek-MultiFlo dispenser into 384-well plates containing prespotted library com-

pounds. Prepared plates were then incubated for 72 h at 37 °C in 5% CO₂, 80% humidity. Reference thick film smears from select control wells were made prior to sealing each plate in aluminum foil and storing at −80 °C for 24 h. Plates were thawed at room temperature (RT), and all ensuing steps were conducted under reduced light. SYBR Green stock solution was prepared by mixing σ -SYBR Green I nucleic acid gel stock (1.2 μ L) into 1 mL of lysis buffer (80 mM Tris-HCl pH 7.52, 20 mM EDTA, 0.032% w/v Saponin, 0.32% v/v 100% Triton X-100). SYBR Green stock solution (15 μ L) was dispensed into each well of the assay plates, and plates were sealed in aluminum foil and stored in the dark for 4 h at RT. Fluorescence was measured by detecting emission at 535 nm after excitation at 485 nm using a BioTek Synergy H1 hybrid reader. Data were fitted to the log(inhibitor) versus response—variable slope (four parameters) model in Graph Pad Prism to determine the effective concentration that led to a 50% reduction in parasitemia (EC₅₀).

Phenotypic Screen Chemical Library. The chemical library used for the screen is an 8K subset of the UT Southwestern compound collection assembled with support from computational chemists at Chemical Diversity Inc (Chem Div) to represent a plate-based diversity subset of our 200K chemical library. Compounds in this subset are compliant with a relaxed set of Lipinski's rules, with 99% having a molecular weight less than 550. The abovementioned SYBR Green assay was optimized on our HTS core platforms as a readout for *P. falciparum* growth using the 384-well plate format. Z' was evaluated as a measure of assay robustness where a $Z' > 0.5$ represents a robust assay. Hits were identified based on an RZ score cutoff of < -3 , where the RZ score represents the number of RSDs that a measurement for a library compound is from the corrected robust median, which is determined after correction for systematic errors (plate, row, and column effects) as described.^{28,29}

Pf Drug-Resistant Laboratory Strains and Cross-Resistance Testing. Drug sensitivity testing was performed using the modified [³H]-hypoxanthine incorporation assay, as previously reported.⁷²

HepG2 In Vitro Cytotoxicity Evaluation. Cytotoxicity was evaluated against HepG2 human hepatoma cell suspensions in the σ -EMEM medium supplemented with 5% heat inactivated fetal bovine serum (Gibco) and 2 mM glutamine. Compounds were dispensed into 384-well plates using a Labcyte Echo555 acoustic dispenser. Methotrexate (Sigma) and 0.5% DMSO were used as positive and negative controls, respectively. All wells were normalized to an upper limit of 0.5% DMSO. A volume of 60 μ L/well was added using a BioTek-MultiFlo dispenser from a 10,000 cells/mL cell suspension preparation of HepG2 cells for a final seeding density of 600 cells/well. Plates were then incubated for 72 h in a humidity chamber at 37 °C, 5% CO₂, and 80% humidity. Cell viability was established by quantifying intracellular ATP using a luciferase-coupled ATP quantification assay (Promega-CellTiter Glo) following the manufacturer's instructions. Data were fitted to the log(inhibitor) vs response—variable slope (four parameters) model in Graph Pad Prism to determine the cytotoxic concentration that led to 50% reduction in the signal (CC₅₀).

***P. falciparum* Relative Rate of Kill Bioluminescence Assay (BRRoK).** The parasite kill rate was estimated as previously described³⁵ using a transgenic luciferase-expressing *P. falciparum* strain, NF54-luc³⁶ (BEI Resources) that had the advantage of expressing luciferase throughout the asexual life cycle. Cultures were maintained in WR99210 (5 nM), but the drug was removed by washing and replating in drug-free media for 2 days prior to the kill rate studies. Briefly, NF54-luc cultures were sequentially synchronized to ring stages using 5% D-sorbitol as described.⁷³ The assay was then conducted with trophozoite stage cultures (20–26 h postinvasion) at 2% parasitaemia and 4% haematocrit. NF54-luc parasites (200 μ L/well) were added to 96-well plates at 2% haematocrit and 2% parasitemia. Triplicate concentrations (30 \times EC₅₀ to 0.33 \times EC₅₀) of benchmark antimalarials and experimental compounds were added to each well and then incubated for 6 h at 37 °C, 5% CO₂, and 80% humidity. Culture samples (40 μ L/well) were then transferred to a white-clear bottom 96-well plate, and parasite viability was determined by luciferase quantification using a luciferase bioluminescence assay (Promega-Luciferase Assay system).

Two-Color Flow Cytometry Kill Rate Assay. Double-colorimetric FACS analysis was used to quantify invasion of prestained human RBCs by drug-treated parasites as described.⁴¹ Briefly, killing profiles were estimated by culturing unlabeled RBCs infected with *P. falciparum* 3D7 parasites in the presence of compounds at 10 \times EC₅₀ for 24 or 48 h. The initial % parasitemia was 0.5% with a hematocrit of 2%. Compound EC₅₀ was determined prior to the start of the study using the 48 h *in vitro* ³H-hypoxanthine incorporation assay as described³⁴ for parasites cultured in standard RPMI 1640 media supplemented with 25 mM HEPES and 0.225% NaHCO₃ supplemented with 2% D-sucrose, 0.3% L-glutamine, 0.005 mM hypoxanthine, and 0.5% AlbuMax II. Culture media for the kill rate study was identical but contained 0.15 mM hypoxanthine. After drug treatment, compounds were removed and infected RBCs were diluted using fresh RBCs previously labeled with carboxylfluorescein diacetate succinimidyl ester (10 μ M for 30 min at 37 °C). Following a further 48 h incubation under standard conditions, the ability of treated parasites to establish infection in fresh labeled RBCs was detected by two-color flow cytometry after labeling parasite DNA with Hoechst 33342 solution (2 μ M). Parasite viability was measured based on the percentage of infected CFDA-SE-stained RBCs in drug-treated samples versus untreated samples of the initial inocula after 48 h incubations with labeled RBCs.

PRR Kill Rate Assay. PRR was assessed using the standard drug washout assay that has been previously described.³⁴ Briefly, parasites were treated with compounds for either 24 or 48 h at 10 \times EC₅₀ (determined as described above) with the compound renewed daily over the treatment period. Parasite samples were removed at the determined time points (0, for the control of the initial number of parasites, 24, and 48 h), the drug was washed out, and drug-free parasites were cultured in 96-well plates after the addition of fresh RBCs and new media in microtiter plates over a threefold serial dilution. Cultures were maintained for up to 28 days to enable parasites to recrudescence. Four independent serial dilutions were carried out with each sample to correct for experimental variation. The number of viable parasites was back-calculated based on X^{n-1} where n is the number of wells where growth was observed and X is the dilution factor.³⁴

Liver-Stage and Gametocidal Assays. *P. berghei* liver-stage assays were performed in the Winzler lab (UCSD) as described.^{19,21} *P. berghei*-ANKA-GFP-Luc-SMCON (Pb-Luc) sporozoites were used to infect HepG2-A16-CD81EGFP cells for this assay, which monitors the ability of compounds to block liver-stage development of luciferase-expressing parasites. Assay media (DMEM without Phenol Red (Life Technology, CA) supplemented with 5% fetal bovine serum, 1.45 mg/mL glutamine, 500 units of penicillin, and 500 μ g/mL streptomycin) was used for the *Pbluc* and *HepG2tox* assays.

Gametocyte assays measuring the viability of mature stage V gametocytes were conducted to determine the ability of compounds to block formation of male and female gametes in the Baum lab (Imperial College, London) as described.^{74–76} The assay identifies compounds that either kill stage V gametocytes, cause sterilization, or interfere with the process of gamete formation.

In Vitro Heme Polymerization Assay. Lipid-mediated H₂ formation was quantified by measuring the formation of β H from hematin, in a detergent-mediated assay that substitutes neutral lipids for the commercially available lipophilic detergent Nonidet P-40 (NP-40).⁷⁷ Unreacted hematin was detected through the formation of the bis-pyridyl-Fe(III)PPIX complex which absorbs at a wavelength of 405 nm. Compound stocks (20 mM) of 3-derivatives (**3**, **9**, and **10**) and pyrimethamine were prepared in DMSO, while CQ was prepared in water. These stocks were then diluted to 2 mM with a water/NP40 detergent solution, resulting in a final solution of compound in 61.1 mM NP40/10% DMSO. Solubility of **3**, **9**, and **10** to 2 mM in this buffer was confirmed (see *in vitro* ADME methods section). Serial dilutions into this same buffer were then made for each compound. A 25 mM hematin stock solution was prepared by sonicating hemin in DMSO for 1 min and then suspending 179 μ L of this stock in a 1 M acetate buffer (20 mL, pH 4.8). The homogenous suspension was then added to the wells to give final buffer and hematin concentrations of 0.5 M and 100 mM, respectively. Plates were covered and incubated at 37 °C for 5 h. A solution of 50% (v/v) pyridine, 30% (v/v) H₂O, 20% (v/v) acetone,

and 2 M HEPES buffer (pH 7.4) was prepared, and 32 μ L of the solution was added to each well to give a final pyridine concentration of 5% (v/v). Acetone (60 μ L) was then added to each well to assist with hematin dispersion. The UV–vis absorbance of the plate wells was read on a SpectraMax P340 plate reader. Sigmoidal concentration–response curves were fitted to the absorbance data using GraphPad Prism version 8 to obtain a 50% inhibitory concentration (IC_{50}) for each compound.

Cellular Heme Polymerization Assay. Inhibition of Hz formation was measured in cultured ABS PfNF54 parasites through a heme fractionation assay,^{53,78} where both % “free” heme and levels of “free” heme-Fe were quantified in femtogram per cell (fg/cell) using a heme standard curve from the mass of each heme-Fe species per trophozoite. Percent free heme and amounts of free heme-Fe were quantified over a range of drug concentrations (0.5–3 \times EC_{50}) and compared to the vehicle control. Briefly, early ring-stage NF54 parasites were treated with a combination of successive sorbitol and Percoll treatments to prepare young rings synchronized to within 3 h postinvasion.⁷⁹ Young rings were incubated with the test drugs at various multiples of their IC_{50} values with a no-drug control included (culture conditions and media as described above). After 32 h, late trophozoites/early schizonts were harvested by lysis of the RBCs with 0.05% saponin followed by multiple washes with 1 \times PBS (pH 7.5) to remove traces of the RBC hemoglobin. Pellets were then resuspended in 1 \times PBS (pH 7.5). An aliquot of the trophozoite suspension was used to quantify, using flow cytometry, the total number of trophozoites isolated. Contents of the remaining trophozoite pellet were then released by hypotonic lysis and sonication. Following centrifugation, treatment with HEPES buffer (pH 7.4), sodium dodecyl sulfate, pyridine, and NaOH, the fractions corresponding to digested hemoglobin, “free” heme, and Hz were carefully recovered. The UV–visible spectrum of each heme fraction as an Fe(III)heme–pyridine complex was measured using a multiwell plate reader (Spectramax 340PC; Molecular Devices). The total amount of each heme species was quantified using a heme standard curve whereby the mass of each heme-Fe species per trophozoite (fg/cell) was calculated by dividing the total amount of each heme species by the corresponding number of parasites in that fraction as determined by flow cytometry. Statistical comparisons and analyses for trends were made on GraphPad Prism version 8 using Students’ *t*-test (GraphPad Software Inc., La Jolla, CA, USA).

In Vitro Selection of Drug-Resistant *P. falciparum* Lines. *P. falciparum* 3D7 parasites (clone A10) resistant to 9 were selected using previously described methods for single-step drug selections.⁸⁰ Briefly, the EC_{50} of 9 versus 3D7-A10 (genetically homogenous clonal line) ring-stage parasites (0.2% parasitemia and 1% hematocrit, cultured in RPMI-1640 media supplemented with 0.5% Albumax) was determined in a 72 h assay for a twofold dilution series (10 points) of 9 (final DMSO concentration was <0.5%) in duplicate along with DMSO solvent controls. Parasite survival was assessed by flow cytometry on an Accuri C6 (BD Biosciences) using SYBR Green and MitoTracker Deep Red FM (Life Technologies) as nuclear stain and vital dyes, respectively. A single-step selection with 2 \times 10⁹ parasites in duplicate was set up at 2% parasitemia and 5% hematocrit using 3 \times EC_{50} of 9 (0.78 μ M). Wells were monitored daily by blood smears until the culture was cleared of live parasites. Drug-containing media was replaced daily until cultures cleared and then every other day thereafter. Cultures were passaged once a week by replacing a fourth of the culture with media and fresh RBCs, with monitoring by blood smears twice a week for up to 60 days to allow for parasite recrudescence.

WGS and Analyses of Drug-Resistant *P. falciparum* Clones. For WGS, genomic DNA was used to prepare libraries using the Illumina Nextera DNA Flex library kit with dual indices, as previously reported.⁸¹ The samples were multiplexed and sequenced on an Illumina MiSeq to obtain 300 bp paired end reads at 19–44 \times depth of coverage across the samples. Sequence reads were aligned to the *P. falciparum* 3D7 genome (PlasmoDB version 36) using BWA (Burrow–Wheeler Alignment). PCR duplicates and unmapped reads were filtered out using Samtools and Picard. The reads were realigned around indels using GATK RealignerTargetCreator, and base quality scores were recalibrated using GATK BaseRecalibrator. GATK HaplotypeCaller

(version 4.1.6) was used to identify any SNVs in clones. These were filtered based on quality scores (variant quality as a function of depth $QD > 1.5$, mapping quality > 40 , and min base quality score > 18) and read depth (depth of read > 5) to obtain high-quality SNPs that were annotated using snpEFF. Comparative SNP analysis between the resistant clones and parent was performed to generate a final list of SNPs that were present exclusively in the resistant clones. BIC-Seq was used to discover CNVs in the resistant mutants against the parent, using the Bayesian statistical model.⁸² Integrated genome viewer was used to visually verify the presence of these SNPs and CNVs in the clones.

ADME: Solubility Measurements. Methods used to assess kinetic solubility in PBS pH 6.5 and pH 2.0 buffers have been previously described.^{25,83} Solubility of 3, 9, and 10 in the buffer used for the *in vitro* heme biomineralization studies was conducted by spiking a 40 μ L aliquot of test compound stock solution into 80 μ L of NP-40 solution followed by 280 μ L of Milli-Q water. The resulting mixtures contained a final compound concentration of 2 mM in 10% (v/v) DMSO and 61.1 mM NP-40. Samples were maintained in a 37 $^{\circ}$ C incubator for the duration of the study. After 1, 2, 4, and 24 h incubations at 37 $^{\circ}$ C, the bulk samples were centrifuged (3 min at 10,000 rpm) and a single aliquot of the supernatant was taken and diluted 20-fold in 50% aqueous acetonitrile for quantitative analysis by HPLC with detection by UV–vis absorbance at 244 nm.

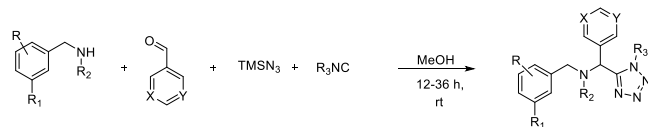
ADME: In Vitro Metabolism and Calculation of Physical Chemical Properties. Compounds (1 μ M) were incubated (up to 60 min at 37 $^{\circ}$ C) with human liver microsomes (Xenotech LLC, Kansas City, KS) at a protein concentration of 0.4 mg/mL with an NADPH regenerating buffer system, as described previously.⁸⁴ Degradation half-life and *in vitro* intrinsic clearance were calculated from the apparent first-order degradation rate constant. Physical–chemical properties were calculated using the ChemAxon chemistry cartridge via JChem for Excel software (version 16.4.11).

Chemical Methods. General. All tested compounds have a purity of >95% as judged by HPLC analysis (UV detection at 210 nm). Chemical shifts δ are in ppm, and spectra were referenced using the residual solvent peak. The following abbreviations are used: singlet (s), doublet (d), triplet (t), quartet (q), double doublet (dd), quintet (quin), multiplet (m), and broad signal (bs). Mass spectra (*m/z*) were recorded on an Agilent LC–MS 1290 Infinity using ESI ionization. All chemicals were used as received unless otherwise noted.

HPLC/MS Analysis. An Agilent 1290 Infinity HPLC system using an Eclipse XDB-C18 column (4.6 \times 150 mm, 5 μ m; Agilent) that was coupled to an Agilent 6130 quadrupole ESI mass spectrometer run in the positive mode with a scan range of 100–1100 *m/z* was used. LC was carried out at a flow rate of 0.5 mL/min at 20 $^{\circ}$ C with a 5 μ L injection volume, using a gradient elution with aqueous acetonitrile containing 0.1% formic acid, 0 min: 30% acetonitrile/water; 0 \rightarrow 6 min: gradient to 95% acetonitrile/water; 6 \rightarrow 12 min 95% acetonitrile/water.

N-(3-Chlorophenyl)-2-(3-methyl-2-oxo-5-phenyl-2,3-dihydro-1*H*-benzof[e][1,4]diazepin-1-yl)butanamide (1). t_R = 9.0 min. ESI-MS (*m/z*): 446.1 [*M* + *H*]⁺.

N-(4-(4-Acetylphenyl)carbamoyl)phenyl)-2,3-dihydrobenzof[b]-[1,4]dioxine-2-carboxamide (2). t_R = 4.24 min. ESI-MS (*m/z*): 417.0 [*M* + *H*]⁺.



General Syntheses of Tetrazole Derivatives.³⁷ Isocyanide (1.0 mmol), aromatic aldehyde (1.0 mmol), *N*-benzylamine (1.0 mmol), and trimethylsilyl azide (1.0 mmol) were dissolved in MeOH (2.0 mL, 2 M) under a N₂ atmosphere. The resulting solution was stirred at RT for 2–3 days. MeOH was evaporated, and the residue was purified by flash column chromatography.

N-(5-Bromo-2-methoxybenzyl)-*N*-methyl-1-phenyl-1-(1-(*o*-tolyl)-1*H*-tetrazol-5-yl)methenamine (3). The target compound was obtained in 73% yield as a colorless thick liquid. ¹H NMR (400 MHz, CDCl₃): δ 7.48–7.42 (m, 2H), 7.33–7.19 (m, 8H), 7.02 (d, *J* = 8.4 Hz,

1H), 6.64 (d, *J* = 8.6 Hz, 1H), 4.94 (s, 1H), 3.69–3.61 (m, 4H), 3.46 (d, *J* = 14.8 Hz, 1H), 2.23 (s, 3H), 1.69 (s, 3H). ¹³C NMR (101 MHz, CDCl₃): δ 156.7, 155.2, 136.0, 135.5, 132.6, 132.1, 131.6, 131.3, 130.6, 129.2, 128.6 (d, *J* = 20.8 Hz), 127.3, 127.0, 113.0, 112.0, 63.3, 55.5, 51.7, 39.6, 17.1. ESI-MS (*m/z*): 478.1 [M + H]⁺. The enantiomers were separated by chiral HPLC (CHIRALCEL OD-H column, 1% isopropanol in hexane, 1.0 mL/min, *t_R* = 25, 32 min). **Enantiomer 1**, [α]_D²⁵ +7.99 (c 0.15, EtOH); **Enantiomer 2**, [α]_D²⁵ −7.99 (c 0.15, EtOH).

N-(2-Methoxybenzyl)-N-methyl-1-phenyl-1-(1-(*o*-tolyl)-1H-tetrazol-5-yl)methanamine (4). The target compound was obtained in 78% yield as a colorless liquid. ¹H NMR (400 MHz, CDCl₃): δ 7.45 (t, *J* = 7.6 Hz, 1H), 7.38–7.25 (m, 8H), 7.20 (t, *J* = 7.8 Hz, 1H), 7.01 (d, *J* = 7.9 Hz, 1H), 6.90 (t, *J* = 7.4 Hz, 1H), 6.80 (d, *J* = 8.2 Hz, 1H), 4.94 (s, 1H), 3.74–3.66 (m, 4H), 3.50 (d, *J* = 14.1 Hz, 1H), 2.26 (s, 3H), 1.73 (s, 3H). ¹³C NMR (101 MHz, CDCl₃): δ 157.6, 155.3, 135.9, 135.7, 132.6, 131.5, 131.1, 129.9, 129.2, 128.4 (d, *J* = 32.0 Hz), 128.1, 127.2, 126.9, 126.5, 120.4, 110.3, 62.9, 55.2, 52.2, 39.2, 17.1. ESI-MS (*m/z*): 400.2 [M + H]⁺.

N-(2-Methoxy-5-(trifluoromethyl)benzyl)-N-methyl-1-phenyl-1-(1-(*o*-tolyl)-1H-tetrazol-5-yl)methanamine (5). The target compound was obtained in 70% yield as a colorless liquid. ¹H NMR (400 MHz, CDCl₃): δ 7.59 (s, 1H), 7.48–7.39 (m, 2H), 7.20–7.31 (m, 7H), 7.00 (d, *J* = 7.7 Hz, 1H), 6.82 (d, *J* = 8.5 Hz, 1H), 4.98 (s, 1H), 3.78–3.70 (m, 4H), 3.52 (d, *J* = 14.8 Hz, 1H), 2.24 (s, 3H), 1.69 (s, 3H). ¹³C NMR (101 MHz, CDCl₃): δ 159.9, 155.0, 135.9, 135.5, 132.5, 131.6, 131.2, 129.1, 128.6 (d, *J* = 16.0 Hz), 127.6, 127.1, 126.9, 126.4 (q, *J* = 15.0 Hz), 125.4 (q, *J* = 16.0 Hz), 122.7 (q, *J* = 131.9 Hz), 109.9, 63.2, 55.5, 51.6, 39.6, 17.1. ESI-MS (*m/z*): 468.2 [M + H]⁺.

N-(2-Methoxy-5-(trifluoromethyl)benzyl)-N-methyl-1-(pyridin-3-yl)-1-(1-(*o*-tolyl)-1H-tetrazol-5-yl)methanamine (6). The target compound was obtained in 63% yield as a white solid. ¹H NMR (400 MHz, CDCl₃): δ 8.56 (dd, *J* = 4.8, 1.6 Hz, 1H), 8.49 (d, *J* = 2.4 Hz, 1H), 7.91 (td, *J* = 8.0, 2.0 Hz, 1H), 7.52–7.44 (m, 3H), 7.38–7.27 (m, 3H), 7.06 (d, *J* = 8.0 Hz, 1H), 6.85 (d, *J* = 8.0 Hz, 1H), 5.03 (s, 1H), 3.73 (s, 3H), 3.71 (d, *J* = 14.8 Hz, 1H), 3.51 (d, *J* = 14.8 Hz, 1H), 2.24 (s, 3H), 1.80 (s, 3H). ¹³C NMR (101 MHz, CDCl₃): δ 159.9, 154.0, 150.3, 149.8, 137.0, 135.6, 132.3, 131.9, 131.5, 131.1, 127.2, 126.9 (d, *J* = 8.68 Hz), 126.6 (q, *J* = 14.4 Hz), 125.8 (q, *J* = 16.0 Hz), 123.5, 122.6 (q, *J* = 134.0 Hz), 110.2, 60.5, 55.5, 51.7, 39.1, 17.2. ESI-MS (*m/z*): 469.3 [M + H]⁺. The enantiomers were separated by chiral HPLC (CHIRALCEL OD-H column, 10% isopropanol in hexane, 1.0 mL/min, *t_R* = 15, 17 min). **Enantiomer 1**, [α]_D²⁵ +5.16 (c 0.15, EtOH); **Enantiomer 2**, [α]_D²⁵ −5.16 (c 0.15, EtOH).

N-(2-Methoxy-5-(trifluoromethyl)benzyl)-N-(pyridin-3-yl)-1-(*o*-tolyl)-1H-tetrazol-5-yl)methyl)cyclopropanamine (7). The target compound was obtained in 61% yield as a colorless liquid. ¹H NMR (400 MHz, CDCl₃): δ 8.55 (m, 2H), 8.08 (d, *J* = 8 Hz, 1H), 7.48–7.20 (m, 6H), 7.00 (d, *J* = 8.0 Hz, 1H), 6.76 (d, *J* = 8.4 Hz, 1H), 5.12 (s, 1H), 4.20 (d, *J* = 12 Hz, 1H), 3.69 (d, *J* = 13.2 Hz, 1H), 3.64 (s, 3H), 1.89 (s, 4H), 0.24–0.15 (m, 2H), −0.05 to −0.11 (m, 1H), −0.29 to −0.39 (m, 1H). ¹³C NMR (101 MHz, CDCl₃): δ 159.9, 153.8, 150.9, 149.8, 137.4, 135.5, 132.3, 131.7, 131.4, 130.2, 129.1 (q, *J* = 14.6 Hz), 127.6, 127.1 (d, *J* = 7.0 Hz), 125.7 (q, *J* = 15.0 Hz), 123.2, 122.2 (q, *J* = 130 Hz), 109.9, 58.5, 55.4, 49.5, 35.1, 17.2, 8.1, 7.5. ESI-MS (*m/z*): 495.1 [M + H]⁺.

N-(2-Fluoro-5-(trifluoromethyl)benzyl)-N-(pyridin-3-yl)-1-(*o*-tolyl)-1H-tetrazol-5-yl)methyl)cyclopropanamine (8). The target compound was obtained in 61% yield as a colorless liquid. ¹H NMR (400 MHz, CDCl₃): δ 8.57 (td, *J* = 4.8, 1.8 Hz, 1H), 8.52 (bs, 1H), 8.01–7.92 (m, 1H), 7.52–7.22 (m, 6H), 7.00 (t, *J* = 8.8 Hz, 2H), 5.19 (s, 1H), 4.27 (d, *J* = 13.8 Hz, 1H), 3.87 (d, *J* = 13.8 Hz, 1H), 1.91 (bs, 4H), 0.35–0.16 (m, 2H), 0.00 to −0.07 (m, 1H), −0.16 to −0.27 (m, 1H). ¹³C NMR (101 MHz, CDCl₃): δ 153.5, 150.7, 150.0, 137.2, 135.5, 132.2, 131.9, 131.5, 130.3, 129.2–129.0 (m), 127.2, 127.0, 123.3, 115.9, 115.7, 58.7, 48.4, 35.2, 17.3, 8.1, 7.7. ESI-MS (*m/z*): 483.1 [M + H]⁺.

N-(Pyridin-3-yl)-1-(*o*-tolyl)-1H-tetrazol-5-yl)methyl)-N-(3-(trifluoromethyl)benzyl)cyclopropanamine (9). The target compound was obtained in 62% yield as a colorless liquid. ¹H NMR (400 MHz, CDCl₃): δ 8.54 (d, *J* = 4.4 Hz, 1H), 8.45 (bs, 1H), 7.83 (d, *J* = 7.2 Hz, 1H), 7.47–7.37 (m, 2H), 7.35–7.18 (m, 6H), 6.88 (d, *J* = 7.2 Hz,

1H), 5.16 (s, 1H), 4.10 (d, *J* = 14.4 Hz, 1H), 3.93 (d, *J* = 14.0 Hz, 1H), 2.05–1.98 (m, 1H), 1.85 (s, 3H), 0.31–0.18 (m, 2H), 0.06 to −0.01 (m, 1H), −0.14 to −0.21 (m, 1H). ¹³C NMR (101 MHz, CDCl₃): δ 153.7, 150.7, 149.9, 140.3, 137.2, 135.5, 132.2 (d, *J* = 20.7 Hz), 131.9, 131.5, 130.9, 130.2 (q, *J* = 135.0 Hz), 128.7, 127.3, 126.9, 125.6 (q, *J* = 15.1 Hz), 123.9 (q, *J* = 14.8 Hz), 123.4, 58.4, 55.6, 35.1, 17.4, 8.9, 7.5. ESI-MS (*m/z*): 465.1 [M + H]⁺.

N-(Pyrimidin-5-yl)-1-(*o*-tolyl)-1H-tetrazol-5-yl)methyl)-N-(3-(trifluoromethyl)benzyl)cyclopropanamine (10). The target compound was obtained in 53% yield as a colorless liquid. ¹H NMR (400 MHz, CDCl₃): δ 9.17 (s, 1H), 8.80 (s, 2H), 7.52–7.43 (m, 2H), 7.40–7.27 (m, 4H), 7.21 (d, *J* = 7.6 Hz, 1H), 6.93 (d, *J* = 7.2 Hz, 1H), 5.16 (s, 1H), 4.07 (d, *J* = 14.0 Hz, 1H), 3.91 (d, *J* = 13.6 Hz, 1H), 2.09–2.01 (m, 1H), 1.90 (s, 3H), 0.39–0.24 (m, 2H), 0.09–0.01 (m, 1H), −0.12 to −0.20 (m, 1H). ¹³C NMR (101 MHz, CDCl₃): δ 158.7, 157.7, 152.5, 139.3, 135.3, 132.2, 132.1, 132.0, 131.8, 130.8 (q, *J* = 130.0 Hz), 128.9, 128.7, 127.4, 126.8, 125.6 (q, *J* = 15.2 Hz), 124.3 (q, *J* = 17.6 Hz), 56.6, 55.8, 35.0, 17.4, 8.9, 7.7. ESI-MS (*m/z*): 466.1 [M + H]⁺.

N-(3-Fluoro-5-(trifluoromethyl)benzyl)-N-(pyrimidin-5-yl)-1-(*o*-tolyl)-1H-tetrazol-5-yl)methyl)cyclopropanamine (11). The target compound was obtained in 51% yield as a colorless liquid. ¹H NMR (400 MHz, CDCl₃): δ 9.18 (s, 1H), 8.81 (s, 2H), 7.50 (t, *J* = 7.2 Hz, 1H), 7.40 (d, *J* = 7.6 Hz, 1H), 7.31 (t, *J* = 7.6 Hz, 1H), 7.15 (d, *J* = 8.0 Hz, 1H), 7.07 (s, 1H), 6.99–6.91 (m, 2H), 5.17 (s, 1H), 4.09 (d, *J* = 14.4 Hz, 1H), 3.91 (d, *J* = 14.4 Hz, 1H), 2.07–1.99 (m, 1H), 1.92 (s, 3H), 0.41–0.26 (m, 2H), 0.12–0.04 (m, 1H), −0.05 to −0.15 (m, 1H). ¹³C NMR (101 MHz, CDCl₃): δ 163.6, 161.2, 158.8, 157.7, 152.4, 142.6 (d, *J* = 25.2 Hz), 135.3, 132.2, 131.9, 131.8, 128.6, 127.5, 126.7, 121.3–121.1 (m), 119.2, 118.9, 112.0 (q, *J* = 18.7 Hz), 111.8 (q, *J* = 15.2 Hz), 56.7, 55.4, 35.3, 17.5, 8.9, 7.7. ESI-MS (*m/z*): 484.0 [M + H]⁺. The enantiomers were separated by chiral HPLC (CHIRALCEL OD-H column, 10% isopropanol in hexane, 1.0 mL/min, *t_R* = 10, 12 min). **Enantiomer 1**, [α]_D²⁵ +24.609 (c 0.195, EtOH); **Enantiomer 2**, [α]_D²⁵ −21.558 (c 0.195, EtOH).

N-(4-Fluoro-3-(trifluoromethyl)benzyl)-N-(pyrimidin-5-yl)-1-(*o*-tolyl)-1H-tetrazol-5-yl)methyl)cyclopropanamine (12). The target compound was obtained in 51% yield as a colorless liquid. ¹H NMR (400 MHz, CDCl₃): δ 9.18 (s, 1H), 8.80 (s, 2H), 7.51 (dt, *J* = 8.0, 1.6 Hz, 1H), 7.40 (d, *J* = 7.6 Hz, 1H), 7.31 (t, *J* = 7.6 Hz, 1H), 7.24–7.18 (m, 2H), 7.03 (t, *J* = 10 Hz, 1H), 6.97 (d, *J* = 8.0 Hz, 1H), 5.16 (s, 1H), 4.06 (d, *J* = 14.0 Hz, 1H), 3.85 (d, *J* = 14.0 Hz, 1H), 2.00–1.88 (m, 4H), 0.39–0.23 (m, 2H), 0.06–0.01 (m, 1H), −0.11 to −0.19 (m, 1H). ¹³C NMR (101 MHz, CDCl₃): δ 158.8, 157.7, 152.4, 135.3, 134.7, 134.6, 134.2, 134.1, 132.1, 131.9, 131.8, 128.7, 127.5, 126.8, 117.0, 116.8, 56.9, 54.9, 35.1, 17.4, 8.8, 7.8. ESI-MS (*m/z*): 484.1 [M + H]⁺.

N-(2-Fluoro-3-(trifluoromethyl)benzyl)-N-(pyrimidin-5-yl)-1-(*o*-tolyl)-1H-tetrazol-5-yl)methyl)cyclopropanamine (13). The target compound was obtained in 50% yield as a colorless liquid. ¹H NMR (400 MHz, CDCl₃): δ 9.20 (s, 1H), 8.88 (s, 2H), 7.52–7.44 (m, 2H), 7.39 (d, *J* = 7.6 Hz, 1H), 7.34–7.27 (m, 2H), 7.11–7.02 (m, 2H), 5.15 (s, 1H), 4.21 (d, *J* = 13.2 Hz, 1H), 3.79 (d, *J* = 13.6 Hz, 1H), 1.97–1.86 (m, 4H), 0.36–0.19 (m, 2H), −0.02 to −0.09 (m, 1H), −0.20 to −0.27 (m, 1H). ¹³C NMR (101 MHz, CDCl₃): δ 158.8, 157.7, 152.5, 135.6 (d, *J* = 11.5 Hz), 135.4, 132.0 (d, *J* = 10.1 Hz), 134.6, 131.7, 128.4, 127.4, 126.9, 126.5 (q, *J* = 11.6 Hz), 123.7 (d, *J* = 11.6 Hz), 57.0, 48.5, 35.0, 17.4, 8.2, 7.9. ESI-MS (*m/z*): 484.1 [M + H]⁺.

N-(Cyclopropyl)-1-(*o*-tolyl)-1H-tetrazol-5-yl)methyl)-N-(3-(trifluoromethyl)benzyl)cyclopropanamine (14). The target compound was obtained in 71% yield as a colorless liquid. ¹H NMR (400 MHz, CDCl₃): δ 7.50–7.42 (m, 2H), 7.40–7.36 (m, 2H), 7.34–7.27 (m, 3H), 7.08 (d, *J* = 6.8 Hz, 1H), 4.17 (d, *J* = 14.4 Hz, 1H), 4.07 (d, *J* = 14.4 Hz, 1H), 3.18 (d, *J* = 10.0 Hz, 1H), 2.13–2.00 (m, 4H), 1.65–1.56 (m, 1H), 0.72–0.64 (m, 1H), 0.61–0.53 (m, 1H), 0.41–0.31 (m, 1H), 0.22–0.09 (m, 2H), −0.03 to −0.12 (m, 1H), −0.21 to −0.37 (m, 2H). ¹³C NMR (101 MHz, CDCl₃): δ 155.9, 141.0, 135.8, 132.8, 132.3, 131.7, 131.2, 130.3 (q, *J* = 127.1 Hz), 128.5, 127.2, 127.0, 125.8 (q, *J* = 14.6 Hz), 123.7 (q, *J* = 14.9 Hz), 62.0, 55.3, 35.4, 17.5, 11.4, 8.5, 6.8, 5.6, 3.9. ESI-MS (*m/z*): 428.1 [M + H]⁺.

N-(Pyrimidin-5-yl)-1-(*o*-tolyl)-1H-tetrazol-5-yl)methyl)-N-(3-(trifluoromethyl)benzyl)acetamide (15). 1-(Pyrimidin-5-yl)-1-(1-(*o*-

tolyl)-1H-tetrazol-5-yl)-N-(3-(trifluoromethyl)benzyl)methanamine was synthesized using (3-(trifluoromethyl)phenyl)methanamine via a general procedure. To a suspension of the abovementioned amine (1.0 mmol) in CH_2Cl_2 was added Et_3N (2.0 mmol) at 0°C . Acetyl chloride (2.0 mmol) was then added dropwise over 5 min. After stirring at RT for 1 h, the mixture was diluted with CH_2Cl_2 and washed with water. The organic layer was dried over anhydrous Na_2SO_4 , and the solvent was evaporated under vacuum. The residue obtained was purified by flash column chromatography (EtOAc /hexane) to furnish the target compound in 51% yield. ^1H NMR (400 MHz, CDCl_3): δ 8.97 (bs, 1H), 8.55 (bs, 2H), 7.55–7.27 (m, 5H), 7.20–6.81 (m, 3H), 5.02 (s, 2H), 2.14 (s, 3H), 1.95 (s, 3H). ^{13}C NMR (101 MHz, CDCl_3): δ 172.2, 159.0, 157.9, 153.2, 137.2, 135.7, 132.2, 131.9, 131.6, 129.7, 129.3–129.2 (m), 127.5, 127.0, 124.6 (q, J = 12.5 Hz), 122.5 (q, J = 16.3 Hz), 49.5, 47.5, 22.2, 17.4. ESI-MS (m/z): 468.0 $[\text{M} + \text{H}]^+$.

N-(2-Fluoro-5-(trifluoromethyl)benzyl)-N-methyl-1-(pyridin-3-yl)-1-(o-tolyl)-1H-tetrazol-5-yl)methanamine (16). The target compound was obtained in 61% yield as a colorless liquid. ^1H NMR (400 MHz, CDCl_3): δ 8.57 (dt, J = 4.8, 1.3 Hz, 1H), 8.45 (d, J = 2.3 Hz, 1H), 7.89 (dt, J = 8.1, 2.0 Hz, 1H), 7.55 (dd, J = 6.6, 2.4 Hz, 1H), 7.53–7.43 (m, 2H), 7.38–7.27 (m, 3H), 7.10–7.00 (m, 2H), 4.98 (s, 1H), 3.74 (d, J = 14.0 Hz, 1H), 3.58 (d, J = 14.1 Hz, 1H), 2.22 (s, 3H), 1.81 (s, 3H). ^{13}C NMR (101 MHz, CDCl_3): δ 164.2, 161.6, 153.9, 150.3 (d, J = 22.7 Hz), 136.9, 135.6, 132.2, 131.9, 131.6, 130.7, 128.1–127.9 (m), 127.3, 126.9, 126.5–126.3 (m), 126.1, 125.2, 125.1, 123.6, 122.4, 116.2, 115.9, 60.5, 50.5 (d, J = 8.8 Hz), 39.0, 17.2. ESI-MS (m/z): 457.1 $[\text{M} + \text{H}]^+$.

1-(1-Cyclohexyl-1H-tetrazol-5-yl)-N-(2-fluoro-5-(trifluoromethyl)benzyl)-N-methyl-1-(pyridin-3-yl)methanamine (17). The target compound was obtained in 62% yield as a colorless liquid. ^1H NMR (400 MHz, CDCl_3): δ 8.69 (d, J = 2.4 Hz, 1H), 8.62 (dd, J = 4.8, 1.2 Hz, 1H), 7.94 (td, J = 8.4, 4.0, 1.6 Hz, 1H), 7.62 (dd, J = 6.4, 2.0 Hz, 1H), 7.57–7.52 (m, 1H), 7.39–7.35 (m, 1H), 7.15 (t, J = 18, 9.6 Hz, 1H), 5.26 (s, 1H), 4.44–4.35 (m, 1H), 3.70 (t, J = 16.0 Hz, 2H), 2.23 (s, 3H), 2.07–1.70 (m, 7H), 1.42–1.23 (m, 3H). ^{13}C NMR (101 MHz, CDCl_3): δ 164.4, 161.9, 152.1, 150.3, 137.2, 130.1, 128.2–128.0 (m), 126.9–126.7 (m), 126.2, 126.1, 125.1, 123.7, 122.4, 116.5, 116.2, 61.2, 58.4, 51.4 (d, J = 8.0 Hz), 38.8, 33.3, 32.9, 25.3 (d, J = 22.1 Hz), 24.8. ESI-MS (m/z): 449.1 $[\text{M} + \text{H}]^+$.

N-((1-Cyclopropyl-1H-tetrazol-5-yl)(pyridin-3-yl)methyl)-N-(3-(trifluoromethyl)benzyl)cyclopropanamine (18). The target compound was obtained in 59% yield as a colorless liquid. ^1H NMR (400 MHz, CDCl_3): δ 8.44 (d, J = 2.4 Hz, 1H), 8.41 (dd, J = 5.2, 1.6 Hz, 1H), 7.73 (td, J = 7.6, 2.0 Hz, 1H), 7.30 (d, J = 7.6 Hz, 1H), 7.23–7.12 (m, 3.5H), 7.07 (s, 0.5H), 5.34 (s, 1H), 3.86 (d, J = 14.0 Hz, 1H), 3.73 (d, J = 14.0 Hz, 1H), 3.12–3.05 (m, 1H), 2.04–1.97 (m, 1H), 1.15–1.05 (m, 1H), 1.00–0.76 (m, 3H), 0.31–0.20 (m, 2H), 0.04 to –0.09 (m, 2H). ^{13}C NMR (101 MHz, CDCl_3): δ 154.3, 150.3, 149.4, 139.9, 138.1, 132.4, 130.7, 128.9, 125.7 (q, J = 14.6 Hz), 124.2 (q, J = 15.2 Hz), 123.6, 58.1, 56.1, 34.7, 28.5, 8.8, 7.7, 7.3, 6.9. ESI-MS (m/z): 415.1 $[\text{M} + \text{H}]^+$.

N-Cyclopropyl-N-((1-cyclopropyl-1H-tetrazol-5-yl)(2-methylpyridin-3-yl)methyl)-1-(3-(trifluoromethyl)phenyl)cyclopropan-1-amine (19). **Step 1: Synthesis of 1-(3-(Trifluoromethyl)phenyl)cyclopropan-1-amine.** Ethylmagnesium bromide (0.7 mL, 2.2 mmol, 3 M in ether) was added to a solution of 3-trifluoromethyl benzonitrile (171 mg, 1.0 mmol) and $\text{Ti}(\text{O}i\text{-Pr})_4$ (312 mg, 1.1 mmol) in Et_2O (5 mL) at -70°C . The yellow solution was stirred for 10 min. After the solution was warmed to RT (1 h), $\text{BF}_3 \cdot \text{OEt}_2$ (292 mg, 2.2 mmol) was added. After the mixture was stirred for 1 h, 1 N HCl (3 mL) and ether (15 mL) were added. NaOH (10% aq, 10 mL) was added to the resulting two clear phases, and the mixture was extracted with ether. The combined ether layers were dried over Na_2SO_4 and concentrated under reduced pressure. The residue was purified by flash column chromatography to furnish the target compound in 63% yield as a colorless oil.

Step 2: Synthesis of N-Cyclopropyl-1-(3-(trifluoromethyl)phenyl)cyclopropan-1-amine. This was synthesized via a general procedure used for synthesis of N-benzylamine.

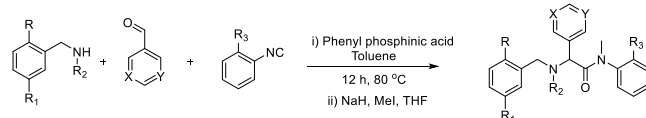
Step 3. The target compound was obtained in 52% yield as a colorless liquid using the general procedure for synthesis of tetrazoles. ^1H NMR (400 MHz, CDCl_3): δ 8.39 (dd, J = 4.8, 1.2 Hz, 1H), 7.47–

7.28 (m, 5H), 7.02 (dd, J = 8.0, 4.8 Hz, 1H), 5.92 (s, 1H), 3.18–3.11 (m, 1H), 2.80–2.73 (m, 1H), 2.47 (s, 3H), 1.49–1.41 (m, 1H), 1.37–1.27 (m, 1H), 1.25–1.16 (m, 2H), 1.06–0.85 (m, 4H), 0.68–0.50 (m, 2H), 0.32–0.23 (m, 1H), –0.24 to –0.33 (m, 1H). ^{13}C NMR (101 MHz, CDCl_3): δ 156.4, 156.0, 148.0, 142.1, 139.0, 132.7, 130.7, 130.2 (q, J = 130 Hz), 128.7, 125.4 (q, J = 14.8 Hz), 124.2 (q, J = 15.6 Hz), 121.3, 56.6, 48.8, 30.5, 28.1, 21.7, 16.7, 13.0, 10.5, 6.8, 6.7, 6.6. ESI-MS (m/z): 455.1 $[\text{M} + \text{H}]^+$.

N-Propyl-N-(pyrimidin-5-yl(1-(o-tolyl)-1H-tetrazol-5-yl)methyl)-1-(3-(trifluoromethyl)phenyl)cyclopropan-1-amine (20). The target compound was obtained in 49% yield as a colorless liquid. ^1H NMR (400 MHz, CDCl_3): δ 9.09 (s, 1H), 8.48 (s, 2H), 7.49 (td, J = 7.6, 1.3 Hz, 1H), 7.39 (dd, J = 10.2, 7.8 Hz, 2H), 7.33–7.24 (m, 3H), 7.16 (s, 1H), 6.87 (d, J = 7.9 Hz, 1H), 5.18 (s, 1H), 2.88 (m, 2H), 1.90 (s, 3H), 1.52–1.34 (m, 2H), 1.18–1.08 (m, 1H), 0.95–0.86 (m, 1H), 0.85–0.78 (m, 1H), 0.71 (t, J = 7.3 Hz, 3H), 0.55–0.48 (m, 1H). ^{13}C NMR (101 MHz, CDCl_3): δ 158.4, 157.2, 154.3, 143.6, 135.1, 132.2, 131.9, 131.8, 131.7, 131.0, 129.0, 127.4, 126.6, 124.3 (q, J = 13.1 Hz), 124.0 (q, J = 14.4 Hz), 55.4, 48.3, 45.8, 23.6, 17.6, 17.2, 11.4. ESI-MS (m/z): 494.2 $[\text{M} + \text{H}]^+$.

N-Propyl-N-(pyridin-3-yl(1-(o-tolyl)-1H-tetrazol-5-yl)methyl)-1-(3-(trifluoromethyl)phenyl)cyclopropan-1-amine (21). The target compound was obtained in 56% yield as a colorless liquid. ^1H NMR (400 MHz, CDCl_3): δ 8.48 (dd, J = 4.8, 1.6 Hz, 1H), 8.21 (d, J = 2.4 Hz, 1H), 7.52–7.36 (m, 3H), 7.34–7.26 (m, 3H), 7.24–7.14 (m, 3H), 6.77 (d, J = 7.2 Hz, 1H), 5.14 (s, 1H), 2.94–2.88 (m, 2H), 1.83 (s, 3H), 1.50–1.27 (m, 2H), 1.20–1.12 (m, 1H), 0.95–0.87 (m, 1H), 0.84–0.77 (m, 1H), 0.70–0.60 (m, 4H). ^{13}C NMR (101 MHz, CDCl_3): δ 155.4, 150.4, 149.6, 144.4, 136.5, 135.2, 133.1, 132.0, 131.4, 130.4 (q, J = 128 Hz), 128.8, 127.2, 126.5, 124.1 (q, J = 14.8 Hz), 123.6 (q, J = 15.2 Hz), 123.2, 57.1, 48.3, 45.7, 23.6, 17.5, 17.0, 11.3. ESI-MS (m/z): 493.1 $[\text{M} + \text{H}]^+$.

General Synthesis of Amide Derivatives.³⁸ Isocyanide (1 mmol), aromatic aldehyde (1 mmol), N-benzylamine (1 mmol), and



phosphinic acid (0.1 mmol) were dissolved in anhydrous toluene (1 mL) under a N_2 atmosphere. The resulting solution was heated at 80°C for 12 h. Toluene was evaporated under reduced pressure, and the residue was purified by flash chromatography.

To a solution of the abovementioned amide (0.5 mmol) in dry tetrahydrofuran was added NaH (0.6 mmol) at 0°C in one portion; then, after 5 min, MeI (1.0 mmol) was added to the reaction mixture at the same temperature. The resulting mixture was allowed to warm at RT and stirred for 30 min. After completion of reaction monitored by LC–MS, the reaction mixture was quenched with cold H_2O , extracted with ethyl acetate, and dried over anhydrous Na_2SO_4 . The organic layer was then concentrated under reduced pressure and purified by flash chromatography.

2-(Cyclopropyl(3-(trifluoromethyl)benzyl)amino)-N-methyl-2-(pyridin-3-yl)-N-(o-tolyl)acetamide (22). The target compound was obtained in 61% yield as a colorless liquid. ^1H NMR (400 MHz, CDCl_3 , 1:1 mixture of rotamers): δ 8.49–8.44 (m, 2H, mixture of rotamers), 8.26 (d, J = 2.3 Hz, 1H, one rotamer), 8.15 (d, J = 2.4 Hz, 1H, one rotamer), 7.63 (dt, J = 7.9, 2.0 Hz, 1H, one rotamer), 7.58 (dt, J = 7.9, 2.0 Hz, 1H, one rotamer), 7.45–7.40 (m, 1H, one rotamer), 7.39–7.31 (m, 4H, mixture of rotamers), 7.25–7.13 (m, 8H, mixture of rotamers), 7.09–7.01 (m, 2H, mixture of rotamers), 6.85 (m, 2H, mixture of rotamers), 6.29 (dd, J = 7.9, 1.3 Hz, 1H, one rotamer), 4.54 (s, 1H, one rotamer), 4.39 (s, 1H, one rotamer), 4.30 (d, J = 14.9 Hz, 1H, one rotamer), 4.24 (d, J = 14.6 Hz, 1H, one rotamer), 3.97 (d, J = 14.7 Hz, 1H, one rotamer), 3.95 (d, J = 14.7 Hz, 1H, one rotamer), 3.23 (s, 3H, one rotamer), 3.19 (s, 3H, one rotamer), 2.36–2.28 (m, 2H, mixture of rotamers), 2.27 (s, 3H, one rotamer), 1.50 (s, 3H, one rotamer), 0.36–0.18 (m, 4H, mixture of rotamers), 0.07 to –0.01 (m, 2H, mixture of rotamers), –0.13 to –0.26 (m, 2H, mixture of rotamers). ^{13}C NMR

(101 MHz, CDCl₃, 1:1 mixture of rotamers): δ 171.5, 171.3, 151.2, 151.0, 149.2, 149.1, 142.5, 141.9, 141.2, 141.1, 137.5, 137.1, 135.8, 135.1, 132.7, 132.0, 131.7, 131.6, 131.5, 131.4, 128.7 (d, J = 13.6 Hz), 128.5 (d, J = 12.0 Hz), 128.2, 128.1, 127.2, 126.9, 125.3 (q, J = 14.4 Hz), 125.1 (q, J = 16.0 Hz), 123.5 (q, J = 16.0 Hz), 123.2 (q, J = 14.4 Hz), 123.1, 123.0, 65.0, 63.5, 56.2, 55.5, 36.2, 35.7, 35.0, 17.5, 16.8, 8.9, 8.7, 7.6, 7.3. ESI-MS (m/z): 454.1 [M + H]⁺.

2-(Cyclopropyl(3-(trifluoromethyl)benzyl)amino)-N-methyl-2-(pyrimidin-5-yl)-N-(o-tolyl)acetamide (23). The target compound was obtained in 45% yield as a colorless liquid. ¹H NMR (400 MHz, MeOD, 1:1 mixture of rotamers): δ 9.04–9.00 (m, 2H, mixture of rotamers), 8.52–8.46 (m, 4H, mixture of rotamers), 7.53–7.22 (m, 11H, mixture of rotamers), 7.18–7.11 (m, 2H, mixture of rotamers), 7.02–6.91 (m, 2H, mixture of rotamers), 6.45 (d, J = 7.8 Hz, 1H, one rotamer), 4.57 (s, 1H, one rotamer), 4.50 (s, 1H, one rotamer), 4.24 (d, J = 14.5 Hz, 1H, one rotamer), 4.18 (d, J = 14.5 Hz, 1H, one rotamer), 4.05–3.98 (m, 2H, mixture of rotamers), 3.25 (s, 3H, one rotamer), 3.21 (s, 3H, one rotamer), 2.38–2.25 (m, 5H, mixture of rotamers), 1.61 (s, 3H, one rotamer), 0.41–0.26 (m, 4H, mixture of rotamers), 0.16–0.05 (m, 2H, mixture of rotamers), –0.07 to –0.15 (m, 1H, one rotamer), –0.16 to –0.24 (m, 1H, one rotamer). ¹³C NMR (101 MHz, MeOD, 1:1 mixture of rotamers): δ 171.9, 171.6, 159.1, 158.9, 158.6, 158.5, 143.2, 142.6, 142.1, 136.5 (d, J = 22.0 Hz), 133.5, 133.2, 132.9, 132.8, 132.3, 131.5, 130.3 (d, J = 21.6 Hz), 130.1, 129.8, 129.5, 129.4, 128.6, 128.0, 126.2 (q, J = 15.2 Hz), 125.9 (q, J = 15.2 Hz), 124.8 (q, J = 16.4 Hz), 124.5 (q, J = 16.4 Hz), 64.4, 63.2, 57.4, 56.9, 36.9, 36.8, 36.7, 36.0, 17.7, 17.0, 9.6, 9.3, 8.5, 8.3. ESI-MS (m/z): 455.2 [M + H]⁺.

2-(Cyclopropyl(3-(trifluoromethylthio)benzyl)amino)-N-methyl-2-(pyridin-3-yl)-N-(o-tolyl)acetamide (24). The target compound was obtained in 59% yield as a colorless liquid. ¹H NMR (400 MHz, CDCl₃, 1:1 mixture of rotamers): δ 8.50–8.45 (m, 2H, mixture of rotamers), 8.27 (d, J = 2.3 Hz, 1H, one rotamer), 8.17 (d, J = 2.4 Hz, 1H, one rotamer), 7.64 (dt, J = 7.9, 2.0 Hz, 1H, one rotamer), 7.57 (dt, J = 7.9, 2.0 Hz, 1H, one rotamer), 7.50–7.30 (m, 4H, mixture of rotamers), 7.25–7.22 (m, 4H, mixture of rotamers), 7.20–7.11 (m, 5H, mixture of rotamers), 7.10–7.00 (m, 2H, mixture of rotamers), 6.93–6.80 (m, 2H, mixture of rotamers), 6.29 (d, J = 7.8 Hz, 1H, one rotamer), 4.55 (s, 1H, one rotamer), 4.39 (s, 1H, one rotamer), 4.27 (d, J = 14.9 Hz, 1H, one rotamer), 4.22 (d, J = 14.5 Hz, 1H, one rotamer), 3.93 (d, J = 14.7 Hz, 1H, one rotamer), 3.91 (d, J = 14.7 Hz, 1H, one rotamer), 3.24 (s, 3H, one rotamer), 3.20 (s, 3H, one rotamer), 2.36–2.29 (m, 2H, mixture of rotamers), 2.26 (s, 3H, one rotamer), 1.52 (s, 3H, one rotamer), 0.34–0.25 (m, 2H, one rotamer), 0.24–0.16 (m, 2H, one rotamer), 0.06 to –0.02 (m, 2H, mixture of rotamer), –0.14 to –0.28 (m, 2H, mixture of rotamer). ¹³C NMR (151 MHz, CDCl₃, 1:1 mixture of rotamers): δ 171.3, 150.4, 150.2, 148.4, 141.1, 138.3, 137.9, 136.5, 136.3, 135.7, 135.1, 134.8, 134.5, 131.7, 131.5, 131.2, 131.0, 130.8, 129.2, 129.0, 128.8, 128.7, 128.4, 128.1, 127.2, 126.9, 123.9, 123.7, 123.3, 123.2, 64.9, 63.4, 56.0, 55.5, 36.3 (d, J = 26.4 Hz), 35.6, 35.0, 17.5, 16.9, 8.8 (d, J = 55.0 Hz), 7.6, 7.2. ESI-MS (m/z): 486.1 [M + H]⁺.

2-(Cyclopropyl(3-(trifluoromethylthio)benzyl)amino)-N-methyl-2-(pyrimidin-5-yl)-N-(o-tolyl)acetamide (25). The target compound was obtained in 46% yield as a colorless liquid. ¹H NMR (400 MHz, CDCl₃, 1:1 mixture of rotamers): δ 9.11–9.08 (m, 2H, mixture of rotamers), 8.50 (s, 2H, one rotamer), 8.48 (s, 2H, one rotamer), 7.51 (dt, J = 7.5, 1.8 Hz, 1H, one rotamer), 7.48–7.38 (m, 2H, mixture of rotamers), 7.36–7.27 (m, 3H, mixture of rotamers), 7.25–7.14 (m, 5H, mixture of rotamers), 7.09–7.00 (m, 2H, mixture of rotamers), 6.89 (td, J = 7.6, 1.7 Hz, 1H, one rotamer), 6.82 (dd, J = 7.8, 1.4 Hz, 1H, one rotamer), 6.33 (dd, J = 7.9, 1.3 Hz, 1H, one rotamer), 4.49 (s, 1H, one rotamer), 4.38 (s, 1H, one rotamer), 4.29 (d, J = 14.8 Hz, 1H, one rotamer), 4.22 (d, J = 14.3 Hz, 1H, one rotamer), 3.92 (d, J = 14.6 Hz, 1H, one rotamer), 3.90 (d, J = 14.6 Hz, 1H, one rotamer), 3.24 (s, 3H, one rotamer), 3.21 (s, 3H, one rotamer), 2.39–2.28 (m, 2H, mixture of rotamers), 2.22 (s, 3H, one rotamer), 1.59 (s, 3H, one rotamer), 0.37–0.27 (m, 2H, one rotamer), 0.27–0.18 (m, 2H, one rotamer), 0.05 to –0.03 (m, 2H, mixture of rotamers), 0.19 to –0.26 (m, 1H, one rotamer), –0.32 to –0.39 (m, 1H, one rotamer). ¹³C NMR (101 MHz, CDCl₃, 1:1 mixture of rotamers): δ 170.3, 170.1, 158.2–157.8 (m),

157.7, 142.4, 141.8, 140.8, 136.4, 136.2, 135.3, 135.2, 135.0, 134.7, 131.7 (d, J = 12.0 Hz), 131.2, 130.9, 130.6, 129.6, 129.4, 129.1 (d, J = 26.0 Hz), 129.0, 128.3, 128.1, 127.3, 127.0, 62.9, 61.6, 56.2, 55.7, 36.3 (d, J = 7.2 Hz), 35.3, 34.5, 17.4, 16.9, 9.1, 8.9, 7.8, 7.5. ESI-MS (m/z): 487.1 [M + H]⁺.

2-(Cyclopropyl(3-(trifluoromethoxy)benzyl)amino)-N-methyl-2-(pyridin-3-yl)-N-(o-tolyl)acetamide (26). The target compound was obtained in 56% yield as a colorless liquid. ¹H NMR (400 MHz, CDCl₃, 1:1 mixture of rotamers): δ 8.50–8.45 (m, 2H, mixture of rotamers), 8.26 (bs, 1H, one rotamer), 8.15 (bs, 1H, one rotamer), 7.62 (dt, J = 7.9, 2.0 Hz, 1H, one rotamer), 7.56 (dt, J = 7.8, 2.0 Hz, 1H, one rotamer), 7.25–7.22 (m, 2H, mixture of rotamers), 7.22–7.11 (m, 5H, mixture of rotamers), 7.10–6.98 (m, 5H, mixture of rotamers), 6.98–6.81 (m, 5H, mixture of rotamers), 6.32–6.25 (m, 1H, one rotamer), 4.54 (s, 1H, one rotamer), 4.38 (s, 1H, one rotamer), 4.26 (d, J = 15.0 Hz, 1H, one rotamer), 4.20 (d, J = 14.7 Hz, 1H, one rotamer), 3.96 (d, J = 14.8 Hz, 1H, one rotamer), 3.94 (d, J = 14.8 Hz, 1H, one rotamer), 3.23 (s, 3H, one rotamer), 3.19 (s, 3H, one rotamer), 2.40–2.29 (m, 2H, mixture of rotamers), 2.25 (s, 3H, one rotamer), 1.49 (s, 3H, one rotamer), 0.36–0.17 (m, 4H, mixture of rotamers), 0.08 to –0.00 (m, 2H, mixture of rotamers), –0.09 to –0.27 (m, 2H, mixture of rotamers). ¹³C NMR (151 MHz, CDCl₃, 1:1 mixture of rotamers): δ 149.1, 148.9, 140.9, 135.5, 135.0, 131.5, 131.4, 129.3 (m), 129.1, 128.8, 128.3, 128.0 (m), 127.2, 126.6 (m), 123.3 (m), 120.7, 119.5, 118.9, 64.6, 63.1, 56.0, 55.4, 36.2, 36.1, 35.5, 34.8, 17.3, 16.7, 8.8, 8.6, 7.1. ESI-MS (m/z): 470.1 [M + H]⁺.

2-(Cyclopropyl(3-(trifluoromethoxy)benzyl)amino)-N-methyl-2-(pyrimidin-5-yl)-N-(o-tolyl)acetamide (27). The target compound was obtained in 43% yield as a colorless liquid. ¹H NMR (400 MHz, CDCl₃, 1:1 mixture of rotamers): δ 9.09 (bs, 2H, mixture of rotamers), 8.48 (s, 2H, one rotamer), 8.47 (s, 2H, one rotamer), 7.30–7.27 (m, 1H, one rotamer), 7.25–7.23 (m, 1H, one rotamer), 7.22–7.14 (m, 3H, mixture of rotamers), 7.12–6.95 (m, 7H, mixture of rotamers), 6.94–6.84 (m, 2H, mixture of rotamers), 6.83–6.76 (m, 1H, one rotamer), 6.32 (dd, J = 7.8, 1.3 Hz, 1H, one rotamer), 4.48 (s, 1H, one rotamer), 4.37 (s, 1H, one rotamer), 4.27 (d, J = 15.0 Hz, 1H, one rotamer), 4.20 (d, J = 14.6 Hz, 1H, one rotamer), 3.96 (d, J = 14.8 Hz, 1H, one rotamer), 3.94 (d, J = 14.8 Hz, 1H, one rotamer), 3.24 (s, 3H, one rotamer), 3.20 (s, 3H, one rotamer), 2.45–2.39 (m, 1H, one rotamer), 2.37–2.32 (m, 1H, one rotamer), 2.22 (s, 3H, one rotamer), 1.57 (s, 3H, one rotamer), 0.41–0.19 (m, 4H, mixture of rotamers), 0.10 to –0.01 (m, 2H, mixture of rotamers), –0.15 to –0.19 (m, 1H, one rotamer), –0.28 to –0.32 (m, 1H, one rotamer). ¹³C NMR (101 MHz, CDCl₃, 1:1 mixture of rotamers): δ 170.4, 170.1, 158.0 (m), 157.7, 143.2, 142.6, 140.9, 135.3, 135.2, 131.7, 130.7, 129.6 (d), 129.3, 129.1, 129.0, 128.3, 128.1, 127.3, 127.0, 126.9, 126.6, 121.0, 120.7, 119.6, 119.2, 62.8, 61.5, 56.3, 55.7, 36.3, 35.4, 34.5, 17.4, 16.9, 9.3, 9.0, 7.8, 7.5. ESI-MS (m/z): 471.1 [M + H]⁺.

2-(Cyclopropyl(3-(trifluoromethyl)benzyl)amino)-N-(2-ethylphenyl)-N-methyl-2-(pyridin-3-yl)acetamide (28). The target compound was obtained in 53% yield as a colorless liquid. ¹H NMR (600 MHz, CDCl₃, 1:1 mixture of rotamers): δ 8.48 (d, J = 4.8 Hz, 2H, mixture of rotamers), 8.24 (s, 1H, one rotamer), 8.19 (s, 1H, one rotamer), 7.73 (s, 1H, one rotamer), 7.63 (d, J = 8.2 Hz, 1H, one rotamer), 7.48–7.27 (m, 7H, mixture of rotamers), 7.27–7.19 (m, 6H, mixture of rotamers), 7.16–7.03 (m, 2H, mixture of rotamers), 6.94–6.81 (m, 2H, mixture of rotamers), 6.28 (d, J = 7.8 Hz, 1H, one rotamer), 4.54 (s, 1H, one rotamer), 4.40 (s, 1H, one rotamer), 4.34 (d, J = 14.8 Hz, 1H, one rotamer), 4.25 (d, J = 14.3 Hz, 1H, one rotamer), 3.95 (s, 1H, one rotamer), 3.93 (s, 1H, one rotamer), 3.25 (s, 3H, one rotamer), 3.22 (s, 3H, one rotamer), 2.69–2.61 (m, 1H, one rotamer), 2.57–2.50 (m, 1H, one rotamer), 2.34–2.24 (m, 2H, mixture of rotamers), 2.05–1.95 (m, 1H, one rotamer), 1.25–1.21 (m, 4H), 0.82 (t, J = 7.6, 1.5 Hz, 3H, one rotamer), 0.38–0.25 (m, 2H, one rotamer), 0.24–0.21 (m, 2H, one rotamer), 0.01 (bs, 2H, mixture of rotamers), –0.189 to –0.24 (m, 2H, mixture of rotamers). ¹³C NMR (151 MHz, CDCl₃): δ 150.1, 150.01, 148.2, 141.4, 140.8, 140.5, 138.5, 138.1, 132.1, 131.7, 129.5, 129.3, 129.1 (d, J = 22.3 Hz), 128.5 (d), 128.3, 128.0, 127.1, 126.7, 125.4, 125.2, 123.4 (d, J = 28.8 Hz), 64.9, 63.3,

56.1, 55.6, 37.1, 37.0, 35.7, 35.1, 29.8, 23.3, 22.8, 14.4, 14.1, 8.7, 8.5, 7.7, 7.5. ESI-MS (m/z): 468.1 $[M + H]^+$.

2-(Cyclopropyl(3-(trifluoromethyl)benzyl)amino)-N-(2-ethylphenyl)-N-methyl-2-(pyrimidin-5-yl)acetamide (29). The target compound was obtained in 42% yield as a colorless liquid. ^1H NMR (400 MHz, CDCl_3 , 1:1 mixture of rotamers): δ 9.08 (bs, 2H, mixture of rotamers), 8.48 (s, 2H, one rotamer), 8.45 (s, 2H, one rotamer), 7.48 (d, $J = 7.3$ Hz, 1H, one rotamer), 7.43–7.25 (m, 10H mixture of rotamers), 7.13 (d, $J = 7.7$ Hz, 1H, one rotamer), 7.05 (t, $J = 7.6$ Hz, 1H, one rotamer), 6.88 (t, $J = 7.6$ Hz, 1H, one rotamer), 6.83 (d, $J = 7.9$ Hz, 1H, one rotamer), 6.32 (d, $J = 7.8$ Hz, 1H, one rotamer), 4.46 (s, 1H, one rotamer), 4.40–4.32 (m, 2H, mixture of rotamers), 4.25 (d, $J = 14.4$ Hz, 1H, one rotamer), 3.94 (d, $J = 14.6$ Hz, 1H, one rotamer), 3.92 (d, $J = 14.6$ Hz, 1H, one rotamer), 3.25 (s, 3H, one rotamer), 3.22 (s, 3H, one rotamer), 2.68–2.57 (m, 1H, one rotamer), 2.52–2.43 (m, 1H, one rotamer), 2.37–2.27 (m, 2H, mixture of rotamers), 2.09–1.99 (m, 1H, one rotamer), 1.36–1.15 (m, 4H, one rotamer), 0.88 (t, $J = 7.6$ Hz, 3H, one rotamer), 0.36–0.20 (m, 4H, mixture of rotamers), 0.09 to –0.01 (m, 2H, mixture of rotamers), –0.20 to –0.27 (m, 1H, one rotamer), –0.29 to –0.39 (m, 1H, one rotamer). ^{13}C NMR (101 MHz, CDCl_3 , 1:1 mixture of rotamers): δ 170.4, 170.1, 158.1, 158.0 (d, $J = 18.0$ Hz), 157.6, 141.7, 141.1 (d, $J = 6.8$ Hz), 140.9, 140.3, 132.0, 131.7, 130.5, 129.7, 129.5 (d, $J = 18.0$ Hz), 128.7, 128.5, 128.4, 128.0, 127.20, 126.9, 125.3 (q, $J = 14.8$ Hz), 125.1 (q, $J = 14.8$ Hz), 123.8 (q, $J = 16.0$ Hz), 123.5 (q, $J = 17.6$ Hz), 62.9, 61.5, 56.3, 55.8, 37.2, 37.1, 35.4, 34.7, 23.3, 22.9, 14.4, 14.3, 9.03, 8.7, 7.9, 7.7. ESI-MS (m/z): 469.1 $[M + H]^+$.

2-(Cyclopropyl(3-(trifluoromethyl)benzyl)amino)-N-methyl-N-phenyl-2-(pyrimidin-5-yl)acetamide (30). The target compound was obtained in 45% yield as a colorless liquid. ^1H NMR (500 MHz, CDCl_3): δ 9.10 (s, 1H), 8.50 (s, 2H), 7.46 (d, $J = 7.5$ Hz, 1H), 7.38 (bs, 1H), 7.36–7.29 (m, 2H), 7.26–7.23 (m, 1H), 7.19 (t, $J = 8.1$ Hz, 2H), 6.72 (s, 2H), 4.53 (s, 1H), 4.16 (d, $J = 14.4$ Hz, 1H), 3.97 (d, $J = 14.5$ Hz, 1H), 3.30 (s, 3H), 2.45–2.40 (m, 1H), 0.37–0.31 (m, 1H), 0.28–0.22 (m, 1H), 0.06–0.0 (m, 1H), –0.24 to –0.30 (m, 1H). ^{13}C NMR (101 MHz, CDCl_3): δ 169.8, 158.1, 157.7, 142.5, 141.1, 132.0, 130.6, 129.8, 128.7, 128.6, 127.2, 125.3 (q, $J = 16.8$ Hz), 123.8 (q, $J = 16.4$ Hz), 61.7, 56.5, 37.6, 34.6, 9.6, 7.2. ESI-MS (m/z): 441.1 $[M + H]^+$.

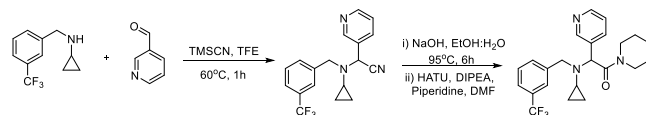
2-(Cyclopropyl(3-(trifluoromethyl)benzyl)amino)-N-methyl-2-(2-methyl-pyrimidin-5-yl)-N-(o-tolyl)acetamide (31). The target compound was obtained in 41% yield as a colorless liquid. ^1H NMR (400 MHz, CDCl_3 , 1:1 mixture of rotamers): δ 8.37 (s, 2H, one rotamer), 8.36 (s, 2H, one rotamer), 7.48–7.44 (m, 1H, one rotamer), 7.41–7.31 (m, 4H, mixture of rotamers), 7.31–7.15 (m, 6H, mixture of rotamers), 7.11–6.99 (m, 2H, mixture of rotamers), 6.92 (td, $J = 7.7$, 1.4 Hz, 1H, one rotamer), 6.84 (d, $J = 8.0$ Hz, 1H, one rotamer), 6.37 (d, $J = 7.8$ Hz, 1H, one rotamer), 4.44 (s, 1H, one rotamer), 4.35 (s, 1H, one rotamer), 4.29 (d, $J = 14.8$ Hz, 1H, one rotamer), 4.23 (d, $J = 14.5$ Hz, 1H, one rotamer), 3.96 (d, $J = 14.6$ Hz, 1H, one rotamer), 3.93 (d, $J = 14.6$ Hz, 1H, one rotamer), 3.23 (s, 3H, one rotamer), 3.20 (s, 3H, one rotamer), 2.70 (d, 6H, mixture of rotamers), 2.37–2.24 (m, 5H, mixture of rotamers), 1.60 (s, 3H, one rotamer), 0.40–0.19 (m, 4H, mixture of rotamers), 0.09 to –0.04 (m, 2H, mixture of rotamers), –0.14 to –0.21 (m, 1H, one rotamer), –0.24 to –0.31 (m, 1H, one rotamer). ^{13}C NMR (101 MHz, CDCl_3 , 1:1 mixture of rotamers): δ 170.6, 170.3, 167.6 (d, $J = 14.8$ Hz), 158.1, 157.8, 141.9, 141.3, 141.0 (d, $J = 14.4$ Hz), 135.4, 135.2, 132.0, 131.7 (d, $J = 27.2$ Hz), 129.0, 128.9, 128.7, 128.4 (d, $J = 28.4$ Hz), 128.1, 127.3, 127.1 (d, $J = 19.2$ Hz), 126.1, 125.3 (q, $J = 13.6$ Hz), 125.1 (q, $J = 15.2$ Hz), 123.7 (q, $J = 15.2$ Hz), 123.4 (d, $J = 16.4$ Hz), 62.7, 61.5, 56.2, 55.7, 36.3 (d, $J = 13.2$ Hz), 35.5, 34.8, 25.8, 17.4, 17.0, 8.9, 8.7, 7.9, 7.6. ESI-MS (m/z): 469.1 $[M + H]^+$.

2-(Cyclopropyl(2-Fluoro-5-(trifluoromethyl)benzyl)amino)-N-methyl-2-(pyridin-3-yl)-N-(o-tolyl)acetamide (32). The target compound was obtained in 46% yield as a colorless liquid. ^1H NMR (400 MHz, CDCl_3 , 1:1 mixture of rotamers): δ 8.48 (m, 2H, mixture of rotamers), 8.32–8.26 (bs, 1H, one rotamer), 8.26–8.21 (bs, 1H, one rotamer), 7.72–7.68 (m, 1H, one rotamer), 7.61–7.57 (m, 1H, one rotamer), 7.45–7.38 (m, 2H, mixture of rotamers), 7.36–7.31 (m, 2H, mixture of rotamers), 7.28–7.26 (m, 1H, one rotamer), 7.24–7.12 (m, 5H, mixture of rotamers), 7.10–7.05 (m, 2H, mixture of rotamers), 7.01 (t, $J = 8.8$ Hz, 1H, one rotamer), 6.93 (t, $J = 8.8$ Hz, 1H, one

rotamer), 6.86 (t, $J = 7.6$ Hz, 1H, one rotamer), 6.33 (d, $J = 8.0$ Hz, 1H), 4.56 (s, 1H, one rotamer), 4.45–4.34 (m, 3H, mixture of rotamers), 4.01 (d, $J = 15.1$ Hz, 1H, one rotamer), 3.92 (d, $J = 14.7$ Hz, 1H, one rotamer), 3.24 (d, $J = 1.2$ Hz, 3H, one rotamer), 3.22 (d, $J = 1.2$ Hz, 3H, one rotamer), 2.33–2.18 (m, 5H, mixture of rotamers), 1.59 (s, 3H, one rotamer), 0.40–0.18 (m, 4H, mixture of rotamers), 0.10 to –0.06 (m, 2H, mixture of rotamers), 0.11 to –0.19 (m, 1H, one rotamer), –0.19 to –0.30 (m, 1H, one rotamer). ^{13}C NMR (101 MHz, CDCl_3 , 1:1 mixture of rotamers): δ 171.3, 171.0, 151.2, 150.9, 149.3, 149.2, 141.4, 141.2, 137.5, 137.2, 135.8, 135.2, 132.3, 131.7, 131.5, 131.2, 128.8 (d, $J = 6.4$ Hz), 128.5, 128.2, 127.3, 126.9, 125.7–125.3 (m), 123.0 (d, $J = 21.9$ Hz), 115.7, 115.5, 115.5, 115.3, 65.0, 63.8, 48.6 (d, $J = 8.0$ Hz), 48.2 (d, $J = 9.6$ Hz), 36.3, 36.2, 35.8, 35.4, 17.5, 16.9, 8.3, 8.0, 7.8, 7.3. ESI-MS (m/z): 472.1 $[M + H]^+$.

N-Methyl-2-(propyl(1-(3-(trifluoromethyl)phenyl)cyclopropyl)-amino)-2-(pyridin-3-yl)-N-(o-tolyl)acetamide (33). The target compound was obtained in 42% yield as a colorless liquid. ^1H NMR (400 MHz, CDCl_3 , 1:1 mixture of rotamers): δ 8.46–8.42 (m, 2H, mixture of rotamers), 8.04 (bs, 1H, one rotamer), 8.01 (bs, 1H, one rotamer), 7.51–7.27 (m, 10H, mixture of rotamers), 7.20–6.90 (m, 8H, mixture of rotamers), 6.75 (t, $J = 7.6$ Hz, 1H, one rotamer), 6.12 (d, $J = 7.8$ Hz, 1H, one rotamer), 4.57 (s, 1H, one rotamer), 4.29 (s, 1H, one rotamer), 3.16 (s, 3H, one rotamer), 3.12 (s, 3H, one rotamer), 3.01–2.88 (m, 2H, one rotamer), 2.85–2.68 (m, 2H, one rotamer), 2.22 (s, 3H, one rotamer), 1.46–1.34 (m, 4H), 1.41–1.12 (m, 7H, mixture of rotamers), 1.11–0.99 (m, 2H, one rotamer), 0.89–0.81 (m, 2H, one rotamer), 0.65–0.56 (m, 6H, mixture of rotamers). ^{13}C NMR (101 MHz, CDCl_3 , 1:1 mixture of rotamers): δ 173.1, 172.7, 151.1, 150.9, 148.9, 148.8, 146.4, 146.0, 141.2, 140.9, 137.2, 136.9, 135.9, 134.8, 134.2, 133.1, 131.7, 131.4, 130.6 (d, $J = 29.6$ Hz), 128.83–128.54 (m), 128.1, 127.2, 126.6, 123.6 (m), 123.0–122.8 (m), 64.0, 63.0, 49.0, 45.6, 45.3, 36.5, 36.3, 31.1, 29.8, 23.7 (d, $J = 21.2$ Hz), 18.2, 17.6, 16.8, 15.4, 11.4 (d, $J = 29.2$ Hz). ESI-MS (m/z): 482.1 $[M + H]^+$.

2-(Cyclopropyl(3-(trifluoromethyl)benzyl)amino)-1-(piperidin-1-yl)-2-(pyridin-3-yl)ethan-1-one (34). To a solution of N-(3-



(trifluoromethyl)benzyl)cyclopropanamine (200 mg, 0.92 mmol) in trifluoroethanol (2 mL) was added nicotinaldehyde (90 μL , 0.92 mmol), and the solution was stirred for 30 min at 60 $^{\circ}\text{C}$. The solution was cooled to RT, and TMSCN (0.11 mL, 0.92 mmol) was added. The mixture was stirred at 60 $^{\circ}\text{C}$ for 30 min. The solvent was evaporated under reduced pressure, and the residue was purified by silica gel column chromatography using EtOAc/hexane as the eluent to furnish 2-(cyclopropyl(3-(trifluoromethyl)benzyl)amino)-2-(pyridin-3-yl)-acetone as a colorless liquid in 82% yield.

To a solution of the abovementioned 2-(cyclopropyl(3-(trifluoromethyl)benzyl)amino)-2-(pyridin-3-yl)acetone (100 mg, 0.3 mmol) in EtOH/ H_2O (3:3) was added NaOH (600 mg, 50 mmol), and the mixture was stirred at 95 $^{\circ}\text{C}$ for 6 h. Progress of the reaction was monitored by HPLC/MS. After completion of the reaction, 6 N HCl was added to pH 7, and the aqueous layer was extracted with EtOAc, dried over anhydrous Na_2SO_4 , and concentrated under reduced pressure. The compound was used for the next reaction without any further purification.

To a solution of the abovementioned acid derivative (40 mg, 0.11 mmol) in dry dimethylformamide (2 mL) at 0 $^{\circ}\text{C}$ were added piperidine (12 mg, 13 μL , 0.13 mmol), HATU (52 mg, 0.13 mmol), and $i\text{-Pr}_3\text{NEt}$ (39 μL , 0.22 mmol). The reaction mixture was stirred for 15 min at RT, then diluted with ethyl acetate, and washed with water and brine. The organic layer was dried over anhydrous Na_2SO_4 , and the solvent was evaporated under vacuum. The residue obtained was purified by flash column chromatography (MeOH/DCM 1:20) to furnish the desired product in 73% yield as a colorless thick liquid.

^1H NMR (600 MHz, MeOD): δ 8.53 (d, $J = 2.2$ Hz, 1H), 8.46 (dd, $J = 4.9$, 1.6 Hz, 1H), 7.86 (dt, $J = 7.9$, 1.9 Hz, 1H), 7.48 (m, 1H), 7.45–

7.39 (m, 4H), 5.07 (s, 1H), 4.13 (d, $J = 14.5$ Hz, 1H), 3.97 (d, $J = 14.5$ Hz, 1H), 3.69–3.63 (m, 1H), 3.59–3.54 (m, 1H), 3.39–3.32 (m, 1H), 3.24 (m, 1H), 2.37 (m, 1H), 1.70–1.53 (m, 4H), 1.39 (m, 1H), 1.20–1.11 (m, 1H), 0.44–0.37 (m, 1H), 0.36–0.27 (m, 2H), 0.06 to –0.04 (m, 1H). ^{13}C NMR (151 MHz, MeOD): δ 170.6, 151.5, 149.5, 143.1, 139.7, 134.5, 133.5, 131.2 (q, $J = 128$ Hz), 129.8, 126.3 (q, $J = 15.6$ Hz), 125.0, 124.5 (d, $J = 13.2$ Hz), 65.1, 57.3, 47.8, 44.1, 35.9, 27.2, 26.8, 25.2, 9.2, 7.6. ESI-MS (m/z): 418.1 $[\text{M} + \text{H}]^+$.

■ ASSOCIATED CONTENT

SI Supporting Information

The Supporting Information is available free of charge at <https://pubs.acs.org/doi/10.1021/acs.jmedchem.0c02022>.

EC₅₀ values against NF54-luc *P. falciparum* parasites; EC₅₀ values associated with cellular heme fractionation; free heme and Hz levels in drug-treated NF54 parasites; whole-genome sequence metrics from Illumina MiSeq (300 bp paired end reads) for the four 9-resistant 3D7 clones; CNVs identified in 9-resistant 3D7 clones; SNPs observed in 9-resistant 3D7 resistant clones; relative rate of kill versus control antimalarials; reduced efficacy of 3-analogues containing 5-Pyr on Dd2 compared to 3D7; snapshots from Integrated Genomics Viewer showing CNVs; and NMR spectra for compounds 3–34 (PDF)

Molecular formula strings (CSV)

■ AUTHOR INFORMATION

Corresponding Authors

Joseph M. Ready – Department of Biochemistry, University of Texas Southwestern Medical Center, Dallas, Texas 75390, United States; orcid.org/0000-0003-1305-9581; Email: joseph.ready@utsouthwestern.edu

Margaret A. Phillips – Department of Biochemistry, University of Texas Southwestern Medical Center, Dallas, Texas 75390, United States; orcid.org/0000-0001-5250-5578; Email: margaret.phillips@utsouthwestern.edu

Authors

Aloysius Lawong – Department of Biochemistry, University of Texas Southwestern Medical Center, Dallas, Texas 75390, United States

Suraksha Gahalawat – Department of Biochemistry, University of Texas Southwestern Medical Center, Dallas, Texas 75390, United States

John Okombo – Department of Microbiology and Immunology, Columbia University Irving Medical Center, New York 10032, United States

Josefine Striepen – Department of Microbiology and Immunology, Columbia University Irving Medical Center, New York 10032, United States

Tomas Yeo – Department of Microbiology and Immunology, Columbia University Irving Medical Center, New York 10032, United States

Sachel Mok – Department of Microbiology and Immunology, Columbia University Irving Medical Center, New York 10032, United States

Ioanna Deni – Department of Microbiology and Immunology, Columbia University Irving Medical Center, New York 10032, United States

Jessica L. Bridgford – Department of Microbiology and Immunology, Columbia University Irving Medical Center, New York 10032, United States

Hanspeter Niederstrasser – Department of Biochemistry, University of Texas Southwestern Medical Center, Dallas, Texas 75390, United States

Anwu Zhou – Department of Biochemistry, University of Texas Southwestern Medical Center, Dallas, Texas 75390, United States

Bruce Posner – Department of Biochemistry, University of Texas Southwestern Medical Center, Dallas, Texas 75390, United States

Sergio Wittlin – Swiss Tropical and Public Health Institute, 4002 Basel, Switzerland; University of Basel, 4002 Basel, Switzerland

Francisco Javier Gamo – Medicines Development Campus, GlaxoSmithKline, 28760 Madrid, Spain; orcid.org/0000-0002-1854-2882

Benigno Crespo – Medicines Development Campus, GlaxoSmithKline, 28760 Madrid, Spain

Alisje Churchyard – Department of Life Sciences, Imperial College London, SW7 2AZ South Kensington, U.K.

Jake Baum – Department of Life Sciences, Imperial College London, SW7 2AZ South Kensington, U.K.

Nimisha Mittal – Division of Host-Microbe Systems and Therapeutics, Department of Pediatrics, University of California San Diego, La Jolla, California 92093, United States

Elizabeth Winzeler – Division of Host-Microbe Systems and Therapeutics, Department of Pediatrics, University of California San Diego, La Jolla, California 92093, United States; orcid.org/0000-0002-4049-2113

Benoît Laleu – Medicines for Malaria Venture, 1215 Geneva, Switzerland; orcid.org/0000-0002-7530-2113

Michael J. Palmer – Medicines for Malaria Venture, 1215 Geneva, Switzerland

Susan A. Charman – Centre for Drug Candidate Optimisation, Monash Institute of Pharmaceutical Sciences, Monash University, Parkville, Victoria 3052, Australia

David A. Fidock – Department of Microbiology and Immunology and Division of Infectious Diseases, Department of Medicine, Columbia University Irving Medical Center, New York 10032, United States

Complete contact information is available at:

<https://pubs.acs.org/doi/10.1021/acs.jmedchem.0c02022>

Author Contributions

A.L. designed, conducted, and analyzed data from the HTS and performed parasite and cytotox assays on synthesized compounds and kill rate studies; S.G. performed synthetic chemistry; J.O. performed heme binding and heme/Hz quantitation assays in drug-treated parasites; J.S., T.Y., S.M., and I.D. performed resistance selections, WGS, or data analysis; H.N., A.Z., and B.P. contributed to the design and implementation of the HTS; S.W., F.J.G., B.C., A.C., J.B., N.M., and E.W. performed parasite assays related to life-cycle profiling and/or kill rate; B.L. and M.J.P. contributed to chemical triage; S.A.C. supervised ADME studies; D.A.F. supervised heme binding and heme/Hz quantitation assays and resistance selections; J.M.R. supervised the medicinal chemistry program; and M.A.P. supervised the HTS and various biological studies. J.M.R. and M.A.P. were responsible for the overall coordination of the project, and they wrote the paper with help from D.A.F. All authors reviewed the manuscript and verified the integrity of their data.

Funding

This work was funded in part by funds from the United States National Institutes of Health grant, R01AI103947 (to M.A.P.), NIGMS predoctoral training grant GM007062 (to A.L.), R37 AI50234 (to D.A.F.), and by Medicines for Malaria Venture through their assay support network to D.A.F., J.B. (RD-08-2800), and E.W.J.B. also holds an Investigator Award from the Wellcome Trust (100993/Z/13/Z). B.P. acknowledges the support of the HTS Core facility by U. T. Southwestern Medical Center and the State of Texas. M.A.P. and J.M.R. acknowledge the support of the Welch Foundation (I-1257, I-1612). M.A.P. holds the Sam G. Winstead and F. Andrew Bell Distinguished Chair in Biochemistry. S.M. is grateful for the support of the Human Frontier Science Program Long-term Postdoctoral Fellowship LT000976/2016-L.

Notes

The authors declare no competing financial interest.

ACKNOWLEDGMENTS

The authors would like to acknowledge the use of the PlasmoDB *Plasmodium* informatics resource as part of the work of this paper. We thank Christian Scheurer for technical assistance with the [³H]-hypoxanthine incorporation assay.

ABBREVIATIONS

MOA, modes of action; ABS, asexual blood stage parasites; ACTs, artemisinin-based combination therapy; CQ, chloroquine; ART, artemisinin; ATQ, atovaquone; MFQ, mefloquine; LUM, lumefantrine; PPQ, piperaquine; WGS, whole genome sequencing; SAR, structure–activity relationships; Hz, hemozooin; β H, β -hematin; DV, digestive vacuole; BRoK, bioluminescence relative rate of kill; DGFA, dual gamete formation assay; PfCRT, *P. falciparum* CQ resistance transporter; CNV, copy number variations; SNPs, single nucleotide polymorphisms

REFERENCES

- (1) World Health Organization. *World Malaria Report*. <https://www.who.int/teams/global-malaria-programme/reports/world-malaria-report-2020>, 2020.
- (2) Phillips, M. A.; Burrows, J. N.; Manyando, C.; van Huijsduijnen, R. H.; Van Voorhis, W. C.; Wells, T. N. C. *Malaria. Nat. Rev. Dis. Primers* **2017**, *3*, 17050.
- (3) Hanboonkunupakarn, B.; White, N. J. The threat of antimalarial drug resistance. *Trop Dis Travel Med Vaccines* **2016**, *2*, 10.
- (4) Blasco, B.; Leroy, D.; Fidock, D. A. Antimalarial drug resistance: linking *Plasmodium falciparum* parasite biology to the clinic. *Nat. Med.* **2017**, *23*, 917–928.
- (5) Hanboonkunupakarn, B.; White, N. J. Advances and roadblocks in the treatment of malaria. *Br. J. Clin. Pharmacol.* **2020**, DOI: 10.1111/bcp.14474.
- (6) Tilley, L.; Straimer, J.; Gnädig, N. F.; Ralph, S. A.; Fidock, D. A. Artemisinin action and resistance in *Plasmodium falciparum*. *Trends Parasitol.* **2016**, *32*, 682–696.
- (7) Intharabut, B.; Kingston, H. W.; Srinamon, K.; Ashley, E. A.; Imwong, M.; Dhorda, M.; Woodrow, C.; Stepniewska, K.; Silamut, K.; Day, N. P. J.; Dondorp, A. M.; White, N. J. Artemisinin resistance and stage dependency of parasite clearance in *falciparum* malaria. *J. Infect. Dis.* **2019**, *219*, 1483–1489.
- (8) Xie, S. C.; Ralph, S. A.; Tilley, L. K13, the cytosome, and artemisinin resistance. *Trends Parasitol.* **2020**, *36*, 533–544.
- (9) Menard, D.; Dondorp, A. Antimalarial drug resistance: a threat to malaria elimination. *Cold Spring Harbor Perspect. Med.* **2017**, *7*, a025619.

- (10) van der Pluijm, R. W.; Imwong, M.; Chau, N. H.; Hoa, N. T.; Thuy-Nhien, N. T.; Thanh, N. V.; Jittamala, P.; Hanboonkunupakarn, B.; Chutasmit, K.; Saelow, C.; Runjarern, R.; Kaewmok, W.; Tripura, R.; Peto, T. J.; Yok, S.; Suon, S.; Sreng, S.; Mao, S.; Oun, S.; Yen, S.; Amaratunga, C.; Lek, D.; Huy, R.; Dhorda, M.; Chotivanich, K.; Ashley, E. A.; Mukaka, M.; Waithira, N.; Cheah, P. Y.; Maude, R. J.; Amato, R.; Pearson, R. D.; Gonçalves, S.; Jacob, C. G.; Hamilton, W. L.; Fairhurst, R. M.; Tarning, J.; Winterberg, M.; Kwiatkowski, D. P.; Pukrittayakamee, S.; Hien, T. T.; Day, N. P.; Miotto, O.; White, N. J.; Dondorp, A. M. Determinants of dihydroartemisinin-piperaquine treatment failure in *Plasmodium falciparum* malaria in Cambodia, Thailand, and Vietnam: a prospective clinical, pharmacological, and genetic study. *Lancet Infect. Dis.* **2019**, *19*, 952–961.

- (11) Hovlid, M. L.; Winzeler, E. A. Phenotypic screens in antimalarial drug discovery. *Trends Parasitol.* **2016**, *32*, 697–707.

- (12) Burrows, J. N.; Burlot, E.; Campo, B.; Cherbuin, S.; Jeanneret, S.; Leroy, D.; Spangenberg, T.; Waterson, D.; Wells, T. N.; Willis, P. Antimalarial drug discovery - the path towards eradication. *Parasitology* **2014**, *141*, 128–139.

- (13) Rottmann, M.; McNamara, C.; Yeung, B. K. S.; Lee, M. C. S.; Zou, B.; Russell, B.; Seitz, P.; Plouffe, D. M.; Dharia, N. V.; Tan, J.; Cohen, S. B.; Spencer, K. R.; Gonzalez-Paez, G. E.; Lakshminarayana, S. B.; Goh, A.; Suwanarusk, R.; Jegla, T.; Schmitt, E. K.; Beck, H.-P.; Brun, R.; Nosten, F.; Renia, L.; Dartois, V.; Keller, T. H.; Fidock, D. A.; Winzeler, E. A.; Diagana, T. T. Spiroindolones, a potent compound class for the treatment of malaria. *Science* **2010**, *329*, 1175–1180.

- (14) Spillman, N. J.; Allen, R. J. W.; McNamara, C. W.; Yeung, B. K. S.; Winzeler, E. A.; Diagana, T. T.; Kirk, K. Na(+) regulation in the malaria parasite *Plasmodium falciparum* involves the cation ATPase PfATP4 and is a target of the spiroindolone antimalarials. *Cell Host Microbe* **2013**, *13*, 227–237.

- (15) Wu, T.; Nagle, A.; Kuhen, K.; Gagaring, K.; Borboa, R.; Francek, C.; Chen, Z.; Plouffe, D.; Goh, A.; Lakshminarayana, S. B.; Wu, J.; Ang, H. Q.; Zeng, P.; Kang, M. L.; Tan, W.; Tan, M.; Ye, N.; Lin, X.; Caldwell, C.; Ek, J.; Skolnik, S.; Liu, F.; Wang, J.; Chang, J.; Li, C.; Hollenbeck, T.; Tuntland, T.; Isbell, J.; Fischli, C.; Brun, R.; Rottmann, M.; Dartois, V.; Keller, T.; Diagana, T.; Winzeler, E.; Glynn, R.; Tully, D. C.; Chatterjee, A. K. Imidazolopiperazines: hit to lead optimization of new antimalarial agents. *J. Med. Chem.* **2011**, *54*, 5116–5130.

- (16) Meister, S.; Plouffe, D. M.; Kuhen, K. L.; Bonamy, G. M. C.; Wu, T.; Barnes, S. W.; Bopp, S. E.; Borboa, R.; Bright, A. T.; Che, J.; Cohen, S.; Dharia, N. V.; Gagaring, K.; Gettayacamin, M.; Gordon, P.; Groessl, T.; Kato, N.; Lee, M. C. S.; McNamara, C. W.; Fidock, D. A.; Nagle, A.; Nam, T.-g.; Richmond, W.; Roland, J.; Rottmann, M.; Zhou, B.; Froissard, P.; Glynn, R. J.; Mazier, D.; Sattabongkot, J.; Schultz, P. G.; Tuntland, T.; Walker, J. R.; Zhou, Y.; Chatterjee, A.; Diagana, T. T.; Winzeler, E. A. Imaging of *Plasmodium* liver stages to drive next-generation antimalarial drug discovery. *Science* **2011**, *334*, 1372–1377.

- (17) McNamara, C. W.; Lee, M. C. S.; Lim, C. S.; Lim, S. H.; Roland, J.; Nagle, A.; Simon, O.; Yeung, B. K. S.; Chatterjee, A. K.; McCormack, S. L.; Manary, M. J.; Zeeman, A.-M.; Decherer, K. J.; Kumar, T. R. S.; Henrich, P. P.; Gagaring, K.; Ibanez, M.; Kato, N.; Kuhen, K. L.; Fischli, C.; Rottmann, M.; Plouffe, D. M.; Bursulaya, B.; Meister, S.; Rameh, L.; Trappe, J.; Haasen, D.; Timmerman, M.; Sauerwein, R. W.; Suwanarusk, R.; Russell, B.; Renia, L.; Nosten, F.; Tully, D. C.; Kocken, C. H. M.; Glynn, R. J.; Bodenreider, C.; Fidock, D. A.; Diagana, T. T.; Winzeler, E. A. Targeting *Plasmodium* PI(4)K to eliminate malaria. *Nature* **2013**, *504*, 248–253.

- (18) Paquet, T.; Le Manach, C.; Cabrera, D. G.; Younis, Y.; Henrich, P. P.; Abraham, T. S.; Lee, M. C. S.; Basak, R.; Ghidelli-Disse, S.; Lafuente-Monasterio, M. J.; Bantscheff, M.; Ruecker, A.; Blagborough, A. M.; Zakutansky, S. E.; Zeeman, A.-M.; White, K. L.; Shackleford, D. M.; Mannila, J.; Morizzi, J.; Scheurer, C.; Angulo-Barturen, I.; Martínez, M. S.; Ferrer, S.; Sanz, L. M.; Gamero, F. J.; Reader, J.; Botha, M.; Decherer, K. J.; Sauerwein, R. W.; Tungtaeng, A.; Vanachayangkul, P.; Lim, C. S.; Burrows, J.; Witty, M. J.; Marsh, K. C.; Bodenreider, C.; Rochford, R.; Solapure, S. M.; Jiménez-Díaz, M. B.; Wittlin, S.; Charman, S. A.; Donini, C.; Campo, B.; Birkholtz, L.-M.; Hanson, K. K.; Drewes, G.; Kocken, C. H. M.; Delves, M. J.; Leroy, D.; Fidock, D. A.

Waterson, D.; Street, L. J.; Chibale, K. Antimalarial efficacy of MMV390048, an inhibitor of Plasmodium phosphatidylinositol 4-kinase. *Sci. Transl. Med.* **2017**, *9*, ead9735.

(19) Abraham, M.; Gagaring, K.; Martino, M. L.; Vanaerschot, M.; Plouffe, D. M.; Calla, J.; Godinez-Macias, K. P.; Du, A. Y.; Wree, M.; Antonova-Koch, Y.; Eribez, K.; Luth, M. R.; Otilie, S.; Fidock, D. A.; McNamara, C. W.; Winzeler, E. A. Probing the open global health chemical diversity library for multistage-active starting points for next-generation antimalarials. *ACS Infect. Dis.* **2020**, *6*, 613–628.

(20) Almela, M. J.; Lozano, S.; Lelièvre, J.; Colmenarejo, G.; Coterón, J. M.; Rodrigues, J.; Gonzalez, C.; Herreros, E. A New set of chemical starting points with plasmodium falciparum transmission-blocking potential for antimalarial drug discovery. *PLoS One* **2015**, *10*, e0135139.

(21) Antonova-Koch, Y.; Meister, S.; Abraham, M.; Luth, M. R.; Otilie, S.; Lukens, A. K.; Sakata-Kato, T.; Vanaerschot, M.; Owen, E.; Jado, J. C.; Maher, S. P.; Calla, J.; Plouffe, D.; Zhong, Y.; Chen, K.; Chaumeau, V.; Conway, A. J.; McNamara, C. W.; Ibanez, M.; Gagaring, K.; Serrano, F. N.; Eribez, K.; Taggard, C. M.; Cheung, A. L.; Lincoln, C.; Ambachew, B.; Rouillier, M.; Siegel, D.; Nosten, F.; Kyle, D. E.; Gamo, F.-J.; Zhou, Y.; Llinás, M.; Fidock, D. A.; Wirth, D. F.; Burrows, J.; Campo, B.; Winzeler, E. A. Open-source discovery of chemical leads for next-generation chemoprotective antimalarials. *Science* **2018**, *362*, eaat9446.

(22) Carolino, K.; Winzeler, E. A. The antimalarial resistome - finding new drug targets and their modes of action. *Curr. Opin. Microbiol.* **2020**, *57*, 49–55.

(23) Ross, L. S.; Fidock, D. A. Elucidating mechanisms of drug-resistant Plasmodium falciparum. *Cell Host Microbe* **2019**, *26*, 35–47.

(24) Llanos-Cuentas, A.; Casapia, M.; Chuquiyauri, R.; Hinojosa, J.-C.; Kerr, N.; Rosario, M.; Toovey, S.; Arch, R. H.; Phillips, M. A.; Rozenberg, F. D.; Bath, J.; Ng, C. L.; Cowell, A. N.; Winzeler, E. A.; Fidock, D. A.; Baker, M.; Möhrle, J. J.; Hooft van Huijsduijnen, R.; Gobeau, N.; Araeipour, N.; Andenmatten, N.; Rückle, T.; Duparc, S. Antimalarial activity of single-dose DSM265, a novel plasmodium dihydroorotate dehydrogenase inhibitor, in patients with uncomplicated Plasmodium falciparum or Plasmodium vivax malaria infection: a proof-of-concept, open-label, phase 2a study. *Lancet Infect. Dis.* **2018**, *18*, 874–883.

(25) Phillips, M. A.; Lotharius, J.; Marsh, K.; White, J.; Dayan, A.; White, K. L.; Njoroge, J. W.; El Mazouni, F.; Lao, Y.; Kokkonda, S.; Tomchick, D. R.; Deng, X.; Laird, T.; Bhatia, S. N.; March, S.; Ng, C. L.; Fidock, D. A.; Wittlin, S.; Lafuente-Monasterio, M.; Benito, F. J. G.; Alonso, L. M. S.; Martinez, M. S.; Jimenez-Diaz, M. B.; Bazaga, S. F.; Angulo-Barturen, I.; Haselden, J. N.; Louttit, J.; Cui, Y.; Sridhar, A.; Zeeman, A.-M.; Kocken, C.; Sauerwein, R.; Decherer, K.; Avery, V. M.; Duffy, S.; Delves, M.; Sinden, R.; Ruecker, A.; Wickham, K. S.; Rochford, R.; Gahagen, J.; Iyer, L.; Riccio, E.; Mirsalis, J.; Bathhurst, L.; Rueckle, T.; Ding, X.; Campo, B.; Leroy, D.; Rogers, M. J.; Rathod, P. K.; Burrows, J. N.; Charman, S. A. A long-duration dihydroorotate dehydrogenase inhibitor (DSM265) for prevention and treatment of malaria. *Sci. Transl. Med.* **2015**, *7*, 296ra111.

(26) Bennett, T. N.; Paguio, M.; Gligorijevic, B.; Seudieu, C.; Kosar, A. D.; Davidson, E.; Roepe, P. D. Novel, rapid, and inexpensive cell-based quantification of antimalarial drug efficacy. *Antimicrob. Agents Chemother.* **2004**, *48*, 1807–1810.

(27) Smilkstein, M.; Sriwilaijaroen, N.; Kelly, J. X.; Wilairat, P.; Riscoe, M. Simple and inexpensive fluorescence-based technique for high-throughput antimalarial drug screening. *Antimicrob. Agents Chemother.* **2004**, *48*, 1803–1806.

(28) Brideau, C.; Gunter, B.; Pikounis, B.; Liaw, A. Improved statistical methods for hit selection in high-throughput screening. *J. Biomol. Screening* **2003**, *8*, 634–647.

(29) Wu, Z.; Liu, D.; Sui, Y. Quantitative assessment of hit detection and confirmation in single and duplicate high-throughput screenings. *J. Biomol. Screening* **2008**, *13*, 159–167.

(30) Baell, J. B.; Nissink, J. W. M. Seven year itch: pan-assay interference compounds (PAINS) in 2017-utility and limitations. *ACS Chem. Biol.* **2018**, *13*, 36–44.

(31) Lipinski, C. A. Drug-like properties and the causes of poor solubility and poor permeability. *J. Pharmacol. Toxicol. Methods* **2000**, *44*, 235–249.

(32) Burrows, J. N.; Duparc, S.; Gutteridge, W. E.; Hooft van Huijsduijnen, R.; Kaszubska, W.; Macintyre, F.; Mazzuri, S.; Mohrle, J. J.; Wells, T. N. C. New developments in anti-malarial target candidate and product profiles. *Malar. J.* **2017**, *16*, 26.

(33) Corey, V. C.; Lukens, A. K.; Istvan, E. S.; Lee, M. C. S.; Franco, V.; Magistrado, P.; Coburn-Flynn, O.; Sakata-Kato, T.; Fuchs, O.; Gnädig, N. F.; Goldgof, G.; Linares, M.; Gomez-Lorenzo, M. G.; De Cozar, C.; Lafuente-Monasterio, M. J.; Prats, S.; Meister, S.; Tanaseichuk, O.; Wree, M.; Zhou, Y.; Willis, P. A.; Gamo, F. J.; Goldberg, D. E.; Fidock, D. A.; Wirth, D. F.; Winzeler, E. A. A broad analysis of resistance development in the malaria parasite. *Nat. Commun.* **2016**, *7*, 11901.

(34) Sanz, L. M.; Crespo, B.; De-Cózar, C.; Ding, X. C.; Llergo, J. L.; Burrows, J. N.; García-Bustos, J. F.; Gamo, F.-J. P. falciparum in vitro killing rates allow to discriminate between different antimalarial mode-of-action. *PLoS One* **2012**, *7*, e30949.

(35) Ullah, I.; Sharma, R.; Biagini, G. A.; Horrocks, P. A validated bioluminescence-based assay for the rapid determination of the initial rate of kill for discovery antimalarials. *J. Antimicrob. Chemother.* **2017**, *72*, 717–726.

(36) Vaughan, A. M.; Mikolajczak, S. A.; Camargo, N.; Lakshmanan, V.; Kennedy, M.; Lindner, S. E.; Miller, J. L.; Hume, J. C. C.; Kappe, S. H. I. A transgenic Plasmodium falciparum NF54 strain that expresses GFP-luciferase throughout the parasite life cycle. *Mol. Biochem. Parasitol.* **2012**, *186*, 143–147.

(37) Giustiniano, M.; Pirali, T.; Massarotti, A.; Biletta, B.; Novellino, E.; Campiglia, P.; Sorba, G.; Tron, G. C. A Practical synthesis of 5-aryl-1-aryltetrazoles using an Ugi-like 4-component reaction followed by a biomimetic transamination. *Synthesis* **2010**, 4107–4118.

(38) Pan, S. C.; List, B. Catalytic three-component Ugi reaction. *Angew. Chem., Int. Ed. Engl.* **2008**, *47*, 3622–3625.

(39) Ferdig, M. T.; Cooper, R. A.; Mu, J.; Deng, B.; Joy, D. A.; Su, X.-z.; Wellems, T. E. Dissecting the loci of low-level quinine resistance in malaria parasites. *Mol. Microbiol.* **2004**, *52*, 985–997.

(40) Wellems, T. E.; Panton, L. J.; Gluzman, I. Y.; do Rosario, V. E.; Gwadz, R. W.; Walker-Jonah, A.; Krogstad, D. J. Chloroquine resistance not linked to mdr-like genes in a Plasmodium falciparum cross. *Nature* **1990**, *345*, 253–255.

(41) Linares, M.; Viera, S.; Crespo, B.; Franco, V.; Gomez-Lorenzo, M. G.; Jimenez-Diaz, M. B.; Angulo-Barturen, I.; Sanz, L. M.; Gamo, F. J. Identifying rapidly parasitocidal anti-malarial drugs using a simple and reliable in vitro parasite viability fast assay. *Malar. J.* **2015**, *14*, 441.

(42) Delves, M.; Plouffe, D.; Scheurer, C.; Meister, S.; Wittlin, S.; Winzeler, E. A.; Sinden, R. E.; Leroy, D. The activities of current antimalarial drugs on the life cycle stages of Plasmodium: a comparative study with human and rodent parasites. *PLoS Med.* **2012**, *9*, e1001169.

(43) Ecker, A.; Lehane, A. M.; Clain, J.; Fidock, D. A. PfCRT and its role in antimalarial drug resistance. *Trends Parasitol.* **2012**, *28*, 504–514.

(44) Kim, J.; Tan, Y. Z.; Wicht, K. J.; Erramilli, S. K.; Dhingra, S. K.; Okombo, J.; Vendome, J.; Hagenah, L. M.; Giacometti, S. I.; Warren, A. L.; Nosol, K.; Roepe, P. D.; Potter, C. S.; Carragher, B.; Kosiakoff, A. A.; Quick, M.; Fidock, D. A.; Mancina, F. Structure and drug resistance of the Plasmodium falciparum transporter PfCRT. *Nature* **2019**, *576*, 315–320.

(45) Dhingra, S. K.; Gabryszewski, S. J.; Small-Saunders, J. L.; Yeo, T.; Henrich, P. P.; Mok, S.; Fidock, D. A. Global spread of mutant PfCRT and its pleiotropic impact on Plasmodium falciparum multidrug resistance and fitness. *mBio* **2019**, *10*, e00303.

(46) Gabryszewski, S. J.; Modchang, C.; Musset, L.; Chookajorn, T.; Fidock, D. A. Combinatorial genetic modeling of pfcr-t-mediated drug resistance evolution in Plasmodium falciparum. *Mol. Biol. Evol.* **2016**, *33*, 1554–1570.

(47) Petersen, I.; Gabryszewski, S. J.; Johnston, G. L.; Dhingra, S. K.; Ecker, A.; Lewis, R. E.; de Almeida, M. J.; Straimer, J.; Henrich, P. P.; Palatulan, E.; Johnson, D. J.; Coburn-Flynn, O.; Sanchez, C.; Lehane, A.

- M.; Lanzer, M.; Fidock, D. A. Balancing drug resistance and growth rates via compensatory mutations in the *Plasmodium falciparum* chloroquine resistance transporter. *Mol. Microbiol.* **2015**, *97*, 381–395.
- (48) Johnson, D. J.; Fidock, D. A.; Mungthin, M.; Lakshmanan, V.; Sidhu, A. B. S.; Bray, P. G.; Ward, S. A. Evidence for a central role for PfCRT in conferring *Plasmodium falciparum* resistance to diverse antimalarial agents. *Mol. Cell* **2004**, *15*, 867–877.
- (49) Ross, L. S.; Dhingra, S. K.; Mok, S.; Yeo, T.; Wicht, K. J.; Kumpornsin, K.; Takala-Harrison, S.; Witkowski, B.; Fairhurst, R. M.; Ariey, F.; Menard, D.; Fidock, D. A. Emerging Southeast Asian PfCRT mutations confer *Plasmodium falciparum* resistance to the first-line antimalarial piperazine. *Nat. Commun.* **2018**, *9*, 3314.
- (50) Fong, K. Y.; Wright, D. W. Hemozoin and antimalarial drug discovery. *Future Med. Chem.* **2013**, *5*, 1437–1450.
- (51) Sullivan, D. J., Jr. Quinolines block every step of malaria heme crystal growth. *Proc. Natl. Acad. Sci. U.S.A.* **2017**, *114*, 7483–7485.
- (52) Bray, P. G.; Mungthin, M.; Ridley, R. G.; Ward, S. A. Access to heme: the basis of chloroquine resistance. *Mol. Pharmacol.* **1998**, *54*, 170–179.
- (53) Combrinck, J. M.; Mabothe, T. E.; Ncokazi, K. K.; Ambele, M. A.; Taylor, D.; Smith, P. J.; Hoppe, H. C.; Egan, T. J. Insights into the role of heme in the mechanism of action of antimalarials. *ACS Chem. Biol.* **2013**, *8*, 133–137.
- (54) Skrzypek, R.; Callaghan, R. The “pushmi-pullyu” of resistance to chloroquine in malaria. *Essays Biochem.* **2017**, *61*, 167–175.
- (55) Valderramos, S. G.; Fidock, D. A. Transporters involved in resistance to antimalarial drugs. *Trends Pharmacol. Sci.* **2006**, *27*, S94–601.
- (56) Sidhu, A. B. S.; Uhlemann, A. C.; Valderramos, S. G.; Valderramos, J. C.; Krishna, S.; Fidock, D. A. Decreasing pfmdr1 copy number in *Plasmodium falciparum* malaria heightens susceptibility to mefloquine, lumefantrine, halofantrine, quinine, and artemisinin. *J. Infect. Dis.* **2006**, *194*, S28–S35.
- (57) Preechapornkul, P.; Imwong, M.; Chotivanich, K.; Pongtavornpinyo, W.; Dondorp, A. M.; Day, N. P. J.; White, N. J.; Pukrittayakamee, S. *Plasmodium falciparum* pfmdr1 amplification, mefloquine resistance, and parasite fitness. *Antimicrob. Agents Chemother.* **2009**, *53*, 1509–1515.
- (58) Guler, J. L.; Freeman, D. L.; Ahyong, V.; Patrapuvich, R.; White, J.; Gujjar, R.; Phillips, M. A.; DeRisi, J.; Rathod, P. K. Asexual populations of the human malaria parasite, *Plasmodium falciparum*, use a two-step genomic strategy to acquire accurate, beneficial DNA amplifications. *PLoS Pathog.* **2013**, *9*, e1003375.
- (59) White, J.; Dhingra, S. K.; Deng, X.; El Mazouni, F.; Lee, M. C. S.; Afanador, G. A.; Lawong, A.; Tomchick, D. R.; Ng, C. L.; Bath, J.; Rathod, P. K.; Fidock, D. A.; Phillips, M. A. Identification and mechanistic understanding of dihydroorotate dehydrogenase point mutations in *Plasmodium falciparum* that confer in vitro resistance to the clinical candidate DSM265. *ACS Infect. Dis.* **2019**, *5*, 90–101.
- (60) Calçada, C.; Silva, M.; Baptista, V.; Thathy, V.; Silva-Pedrosa, R.; Granja, D.; Ferreira, P. E.; Gil, J. P.; Fidock, D. A.; Veiga, M. I. Expansion of a specific *Plasmodium falciparum* PfMDR1 haplotype in Southeast Asia with increased substrate transport. *mBio* **2020**, *11*, e02093.
- (61) Cowman, A. F.; Karcz, S.; Galatis, D.; Culvenor, J. G. A P-glycoprotein homologue of *Plasmodium falciparum* is localized on the digestive vacuole. *J. Cell Biol.* **1991**, *113*, 1033–1042.
- (62) Rohrbach, P.; Sanchez, C. P.; Hayton, K.; Friedrich, O.; Patel, J.; Sidhu, A. B. S.; Ferdig, M. T.; Fidock, D. A.; Lanzer, M. Genetic linkage of pfmdr1 with food vacuolar solute import in *Plasmodium falciparum*. *EMBO J.* **2006**, *25*, 3000–3011.
- (63) Sidhu, A. B. S.; Valderramos, S. G.; Fidock, D. A. pfmdr1 mutations contribute to quinine resistance and enhance mefloquine and artemisinin sensitivity in *Plasmodium falciparum*. *Mol. Microbiol.* **2005**, *57*, 913–926.
- (64) Veiga, M. I.; Dhingra, S. K.; Henrich, P. P.; Straimer, J.; Gnädig, N.; Uhlemann, A. C.; Martin, R. E.; Lehane, A. M.; Fidock, D. A. Globally prevalent PfMDR1 mutations modulate *Plasmodium falciparum* susceptibility to artemisinin-based combination therapies. *Nat. Commun.* **2016**, *7*, 11553.
- (65) de Villiers, K. A.; Marques, H. M.; Egan, T. J. The crystal structure of halofantrine-ferriprotoporphyrin IX and the mechanism of action of arylmethanol antimalarials. *J. Inorg. Biochem.* **2008**, *102*, 1660–1667.
- (66) Gildenhuys, J.; Sammy, C. J.; Müller, R.; Streltsov, V. A.; le Roex, T.; Kuter, D.; de Villiers, K. A. Alkoxide coordination of iron(III) protoporphyrin IX by antimalarial quinoline methanols: a key interaction observed in the solid-state and solution. *Dalton Trans.* **2015**, *44*, 16767–16777.
- (67) Egan, T. J.; Hunter, R.; Kaschula, C. H.; Marques, H. M.; Misplon, A.; Walden, J. Structure-function relationships in amino-quinolines: effect of amino and chloro groups on quinoline-hematin complex formation, inhibition of beta-hematin formation, and antiparasitoid activity. *J. Med. Chem.* **2000**, *43*, 283–291.
- (68) Olafson, K. N.; Nguyen, T. Q.; Rimer, J. D.; Vekilov, P. G. Antimalarials inhibit hematin crystallization by unique drug-surface site interactions. *Proc. Natl. Acad. Sci. U.S.A.* **2017**, *114*, 7531–7536.
- (69) Fong, K. Y.; Sandlin, R. D.; Wright, D. W. Identification of beta-hematin inhibitors in the MMV Malaria Box. *Int. J. Parasitol.: Drugs Drug Resist.* **2015**, *5*, 84–91.
- (70) Kumar, M.; Okombo, J.; Mambwe, D.; Taylor, D.; Lawrence, N.; Reader, J.; van der Watt, M.; Fontinha, D.; Sanches-Vaz, M.; Bezuidenhout, B. C.; Lauterbach, S. B.; Liebenberg, D.; Birkholtz, L.-M.; Coetzer, T. L.; Prudêncio, M.; Egan, T. J.; Wittlin, S.; Chibale, K. Multistage antiplasmodium activity of astemizole analogues and inhibition of hemozoin formation as a contributor to their mode of action. *ACS Infect. Dis.* **2019**, *5*, 303–315.
- (71) Trager, W.; Jensen, J. Human malaria parasites in continuous culture. *Science* **1976**, *193*, 673–675.
- (72) Snyder, C.; Chollet, J.; Santo-Tomas, J.; Scheurer, C.; Wittlin, S. In vitro and in vivo interaction of synthetic peroxide RBx11160 (OZ277) with piperazine in *Plasmodium* models. *Exp. Parasitol.* **2007**, *115*, 296–300.
- (73) Lambros, C.; Vanderberg, J. P. Synchronization of *Plasmodium falciparum* erythrocytic stages in culture. *J. Parasitol.* **1979**, *65*, 418–420.
- (74) Delves, M. J.; Miguel-Blanco, C.; Matthews, H.; Molina, I.; Ruecker, A.; Yahya, S.; Straschil, U.; Abraham, M.; Leon, M. L.; Fischer, O. J.; Rueda-Zubiaurre, A.; Brandt, J. R.; Cortes, A.; Barnard, A.; Fuchter, M. J.; Calderon, F.; Winzeler, E. A.; Sinden, R. E.; Herreros, E.; Gamo, F. J.; Baum, J. A high throughput screen for next-generation leads targeting malaria parasite transmission. *Nat. Commun.* **2018**, *9*, 3805.
- (75) Delves, M. J.; Ruecker, A.; Straschil, U.; Lelièvre, J.; Marques, S.; López-Barragán, M. J.; Herreros, E.; Sinden, R. E. Male and female *Plasmodium falciparum* mature gametocytes show different responses to antimalarial drugs. *Antimicrob. Agents Chemother.* **2013**, *57*, 3268–3274.
- (76) Delves, M. J.; Straschil, U.; Ruecker, A.; Miguel-Blanco, C.; Marques, S.; Dufour, A. C.; Baum, J.; Sinden, R. E. Routine in vitro culture of *P. falciparum* gametocytes to evaluate novel transmission-blocking interventions. *Nat. Protoc.* **2016**, *11*, 1668–1680.
- (77) Ncokazi, K. K.; Egan, T. J. A colorimetric high-throughput beta-hematin inhibition screening assay for use in the search for antimalarial compounds. *Anal. Biochem.* **2005**, *338*, 306–319.
- (78) Combrinck, J. M.; Fong, K. Y.; Gibbard, L.; Smith, P. J.; Wright, D. W.; Egan, T. J. Optimization of a multi-well colorimetric assay to determine haem species in *Plasmodium falciparum* in the presence of anti-malarials. *Malar. J.* **2015**, *14*, 253.
- (79) Straimer, J.; Gnädig, N. F.; Witkowski, B.; Amaratunga, C.; Duru, V.; Ramadani, A. P.; Dacheux, M.; Khim, N.; Zhang, L.; Lam, S.; Gregory, P. D.; Urnov, F. D.; Mercereau-Puijalon, O.; Benoit-Vical, F.; Fairhurst, R. M.; Menard, D.; Fidock, D. A. K13-propeller mutations confer artemisinin resistance in *Plasmodium falciparum* clinical isolates. *Science* **2015**, *347*, 428–431.

- (80) Ng, C. L.; Fidock, D. A. *Plasmodium falciparum* In vitro drug resistance selections and gene editing. *Methods Mol. Biol.* **2019**, *2013*, 123–140.
- (81) Yoo, E.; Schulze, C. J.; Stokes, B. H.; Onguka, O.; Yeo, T.; Mok, S.; Gnädig, N. F.; Zhou, Y.; Kurita, K.; Foe, I. T.; Terrell, S. M.; Boucher, M. J.; Cieplak, P.; Kumpornsin, K.; Lee, M. C. S.; Linington, R. G.; Long, J. Z.; Uhlemann, A.-C.; Weerapana, E.; Fidock, D. A.; Bogoy, M. The antimalarial natural product salinipostin identifies essential α /beta serine hydrolases involved in lipid metabolism in *P. falciparum* parasites. *Cell Chem. Biol.* **2020**, *27*, 143–157.
- (82) Xi, R.; Hadjipanayis, A. G.; Luquette, L. J.; Kim, T.-M.; Lee, E.; Zhang, J.; Johnson, M. D.; Muzny, D. M.; Wheeler, D. A.; Gibbs, R. A.; Kucherlapati, R.; Park, P. J. Copy number variation detection in whole-genome sequencing data using the Bayesian information criterion. *Proc. Natl. Acad. Sci. U.S.A.* **2011**, *108*, E1128–E1136.
- (83) Charman, S. A.; Andreu, A.; Barker, H.; Blundell, S.; Campbell, A.; Campbell, M.; Chen, G.; Chiu, F. C. K.; Crighton, E.; Katneni, K.; Morizzi, J.; Patil, R.; Pham, T.; Ryan, E.; Saunders, J.; Shackleford, D. M.; White, K. L.; Almond, L.; Dickins, M.; Smith, D. A.; Moehrle, J. J.; Burrows, J. N.; Abba, N. An in vitro toolbox to accelerate anti-malarial drug discovery and development. *Malar. J.* **2020**, *19*, 1.
- (84) Kokkonda, S.; Deng, X.; White, K. L.; El Mazouni, F.; White, J.; Shackleford, D. M.; Katneni, K.; Chiu, F. C. K.; Barker, H.; McLaren, J.; Crighton, E.; Chen, G.; Angulo-Barturen, I.; Jimenez-Diaz, M. B.; Ferrer, S.; Huertas-Valentin, L.; Martinez-Martinez, M. S.; Lafuente-Monasterio, M. J.; Chittimalla, R.; Shahi, S. P.; Wittlin, S.; Waterson, D.; Burrows, J. N.; Matthews, D.; Tomchick, D.; Rathod, P. K.; Palmer, M. J.; Charman, S. A.; Phillips, M. A. Lead optimization of a pyrrole-based dihydroorotate dehydrogenase inhibitor series for the treatment of malaria. *J. Med. Chem.* **2020**, *63*, 4929–4956.
- (85) Baragaña, B.; Hallyburton, I.; Lee, M. C. S.; Norcross, N. R.; Grimaldi, R.; Otto, T. D.; Proto, W. R.; Blagborough, A. M.; Meister, S.; Wirjanata, G.; Ruecker, A.; Upton, L. M.; Abraham, T. S.; Almeida, M. J.; Pradhan, A.; Porzelle, A.; Martínez, M. S.; Bolscher, J. M.; Woodland, A.; Luksch, T.; Norval, S.; Zuccotto, F.; Thomas, J.; Simeons, F.; Stojanovski, L.; Osuna-Cabello, M.; Brock, P. M.; Churcher, T. S.; Sala, K. A.; Zakutansky, S. E.; Jiménez-Díaz, M. B.; Sanz, L. M.; Riley, J.; Basak, R.; Campbell, M.; Avery, V. M.; Sauerwein, R. W.; Dechering, K. J.; Noviyanti, R.; Campo, B.; Frearson, J. A.; Angulo-Barturen, I.; Ferrer-Bazaga, S.; Gamo, F. J.; Wyatt, P. G.; Leroy, D.; Siegl, P.; Delves, M. J.; Kyle, D. E.; Wittlin, S.; Marfurt, J.; Price, R. N.; Sinden, R. E.; Winzeler, E. A.; Charman, S. A.; Bebrevska, L.; Gray, D. W.; Campbell, S.; Fairlamb, A. H.; Willis, P. A.; Rayner, J. C.; Fidock, D. A.; Read, K. D.; Gilbert, I. H.; Gilbert, I. H. A novel multiple-stage antimalarial agent that inhibits protein synthesis. *Nature* **2015**, *522*, 315–320.
- (86) Kuhen, K. L.; Chatterjee, A. K.; Rottmann, M.; Gagaring, K.; Borboa, R.; Buenviaje, J.; Chen, Z.; Francek, C.; Wu, T.; Nagle, A.; Barnes, S. W.; Plouffe, D.; Lee, M. C. S.; Fidock, D. A.; Graumans, W.; van de Vegte-Bolmer, M.; van Gemert, G. J.; Wirjanata, G.; Sebayang, B.; Marfurt, J.; Russell, B.; Suwanarusk, R.; Price, R. N.; Nosten, F.; Tungtaeng, A.; Gettayacamin, M.; Sattabongkot, J.; Taylor, J.; Walker, J. R.; Tully, D.; Patra, K. P.; Flannery, E. L.; Vinetz, J. M.; Renia, L.; Sauerwein, R. W.; Winzeler, E. A.; Glynn, R. J.; Diagana, T. T. KAF156 is an antimalarial clinical candidate with potential for use in prophylaxis, treatment, and prevention of disease transmission. *Antimicrob. Agents Chemother.* **2014**, *58*, 5060–5067.
- (87) Miley, G. P.; Pou, S.; Winter, R.; Nilsen, A.; Li, Y.; Kelly, J. X.; Stickles, A. M.; Mather, M. W.; Forquer, I. P.; Pershing, A. M.; White, K.; Shackleford, D.; Saunders, J.; Chen, G.; Ting, L.-M.; Kim, K.; Zakharov, L. N.; Donini, C.; Burrows, J. N.; Vaidya, A. B.; Charman, S. A.; Riscoe, M. K. ELQ-300 prodrugs for enhanced delivery and single-dose cure of malaria. *Antimicrob. Agents Chemother.* **2015**, *59*, 5555–5560.
- (88) Pelleau, S.; Moss, E. L.; Dhingra, S. K.; Volney, B.; Casteras, J.; Gabryszewski, S. J.; Volkman, S. K.; Wirth, D. F.; Legrand, E.; Fidock, D. A.; Neafsey, D. E.; Musset, L. Adaptive evolution of malaria parasites in French Guiana: Reversal of chloroquine resistance by acquisition of a mutation in *pfcrt*. *Proc. Natl. Acad. Sci. U.S.A.* **2015**, *112*, 11672–11677.
- (89) Tse, E. G.; Korsik, M.; Todd, M. H. The past, present and future of anti-malarial medicines. *Malar. J.* **2019**, *18*, 93.
- (90) Phillips, M. A.; Gujjar, R.; Malmquist, N. A.; White, J.; El Mazouni, F.; Baldwin, J.; Rathod, P. K. Triazolopyrimidine-based dihydroorotate dehydrogenase inhibitors with potent and selective activity against the malaria parasite *Plasmodium falciparum*. *J. Med. Chem.* **2008**, *51*, 3649–3653.

NOTE ADDED AFTER ASAP PUBLICATION

After this paper was published ASAP on February 23, 2021, minor changes were made to Table 6. The corrected version was reposted February 25, 2021.